Acyclic Cucurbit[n]uril-Type Molecular Containers: Influence of Glycoluril Oligomer Length on their Function as Solubilizing Agents

Supporting Information

by Laura Gilberg,[†,‡] Ben Zhang,[‡] Peter Y. Zavalij,[‡] Vladimir Sindelar,[,†] and Lyle Isaacs*[,‡]*

[†]Department of Chemistry, Masaryk University, Kamenice 5, 625 00 Brno, Czech Republic,
[‡]Department of Chemistry and Biochemistry, University of Maryland, College Park, Maryland 20742, United States

Table of Contents **Pages**

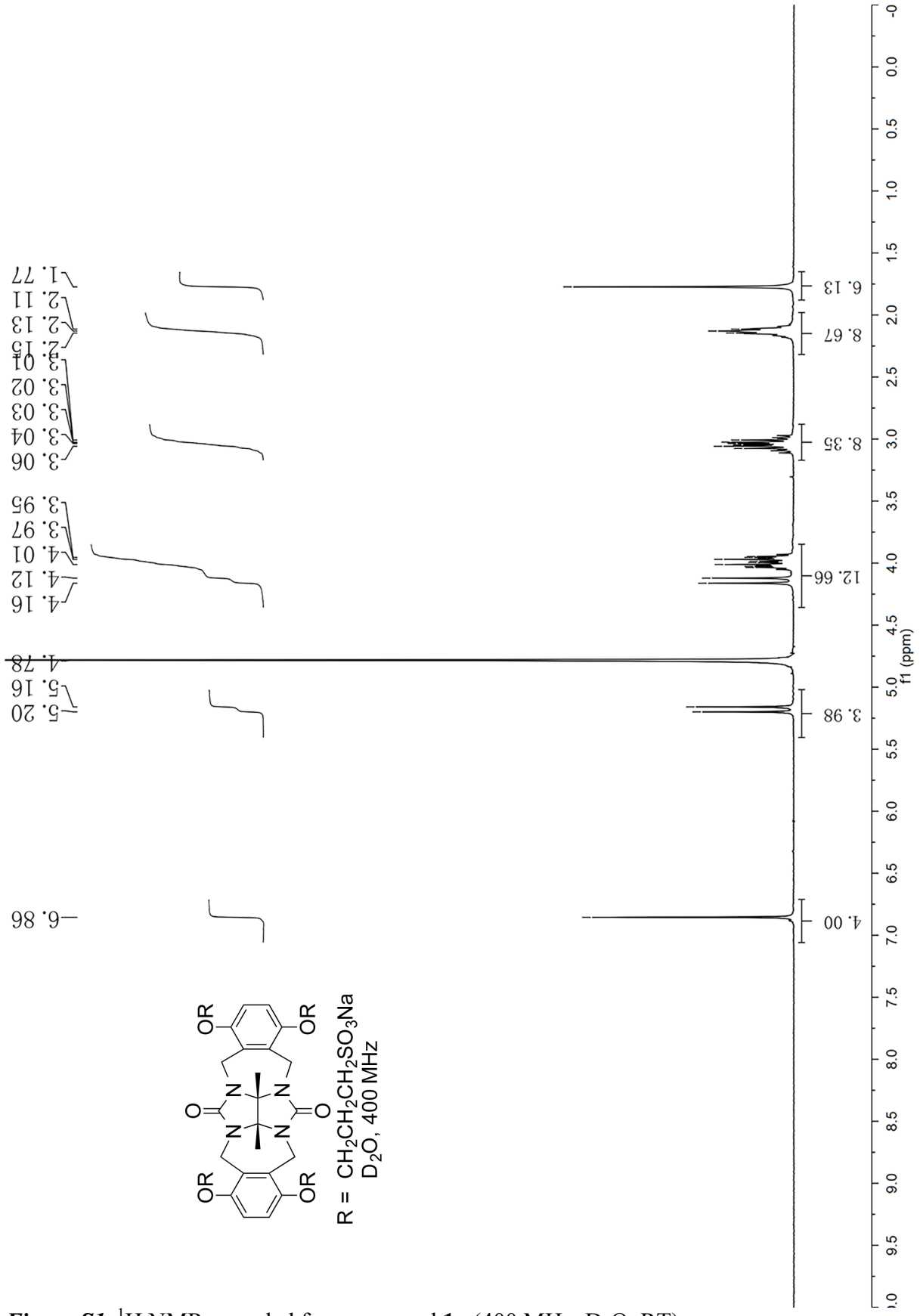

Figure S1. ^{1}H NMR recorded for compound **1a** (400 MHz, D_2O, RT).

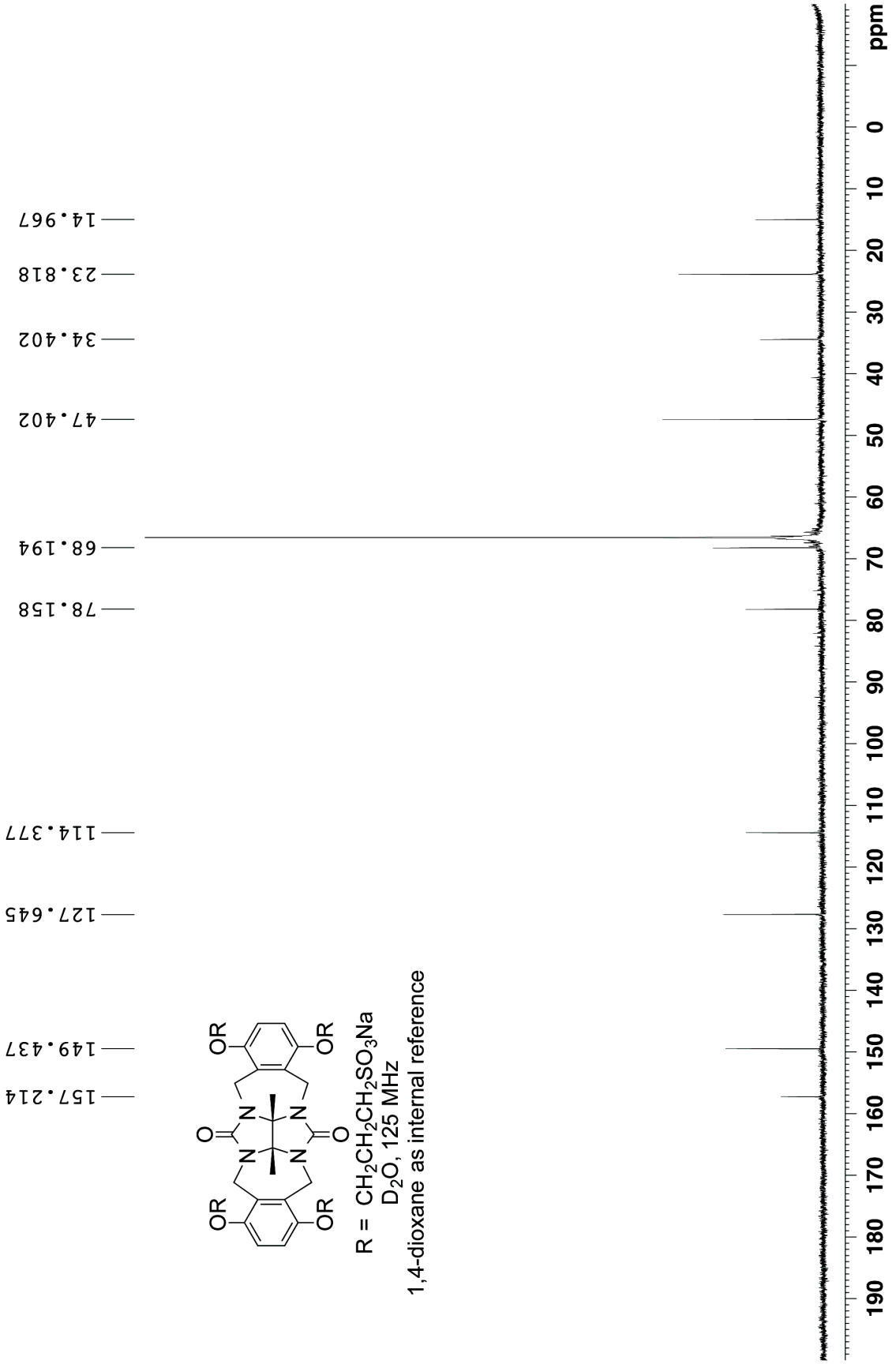

Figure S2. ^{13}C NMR recorded for compound **1a** (125 MHz, D_2O, RT, 1,4-dioxane as internal reference).

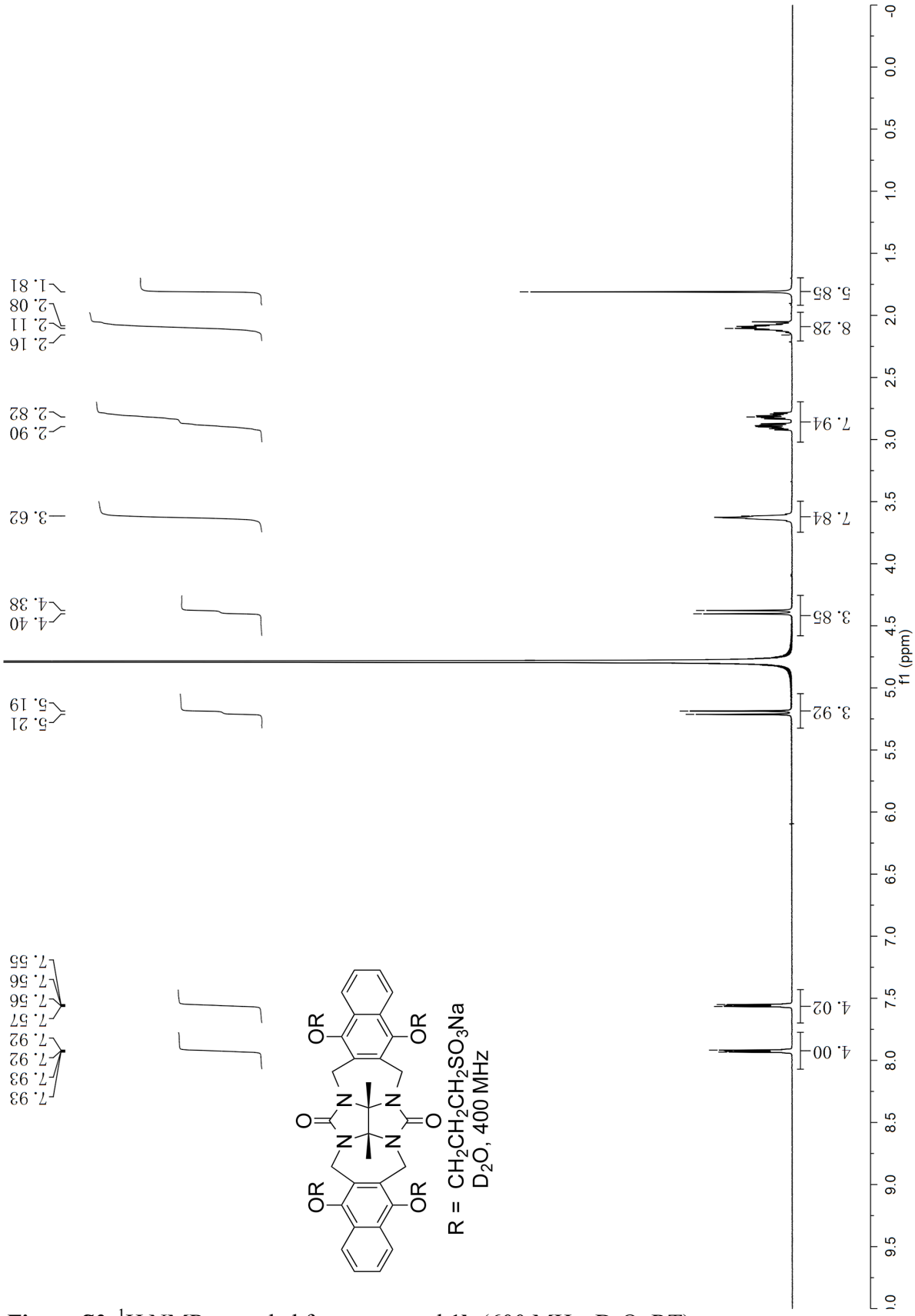

Figure S3. ^{1}H NMR recorded for compound **1b** (600 MHz, D_2O, RT).

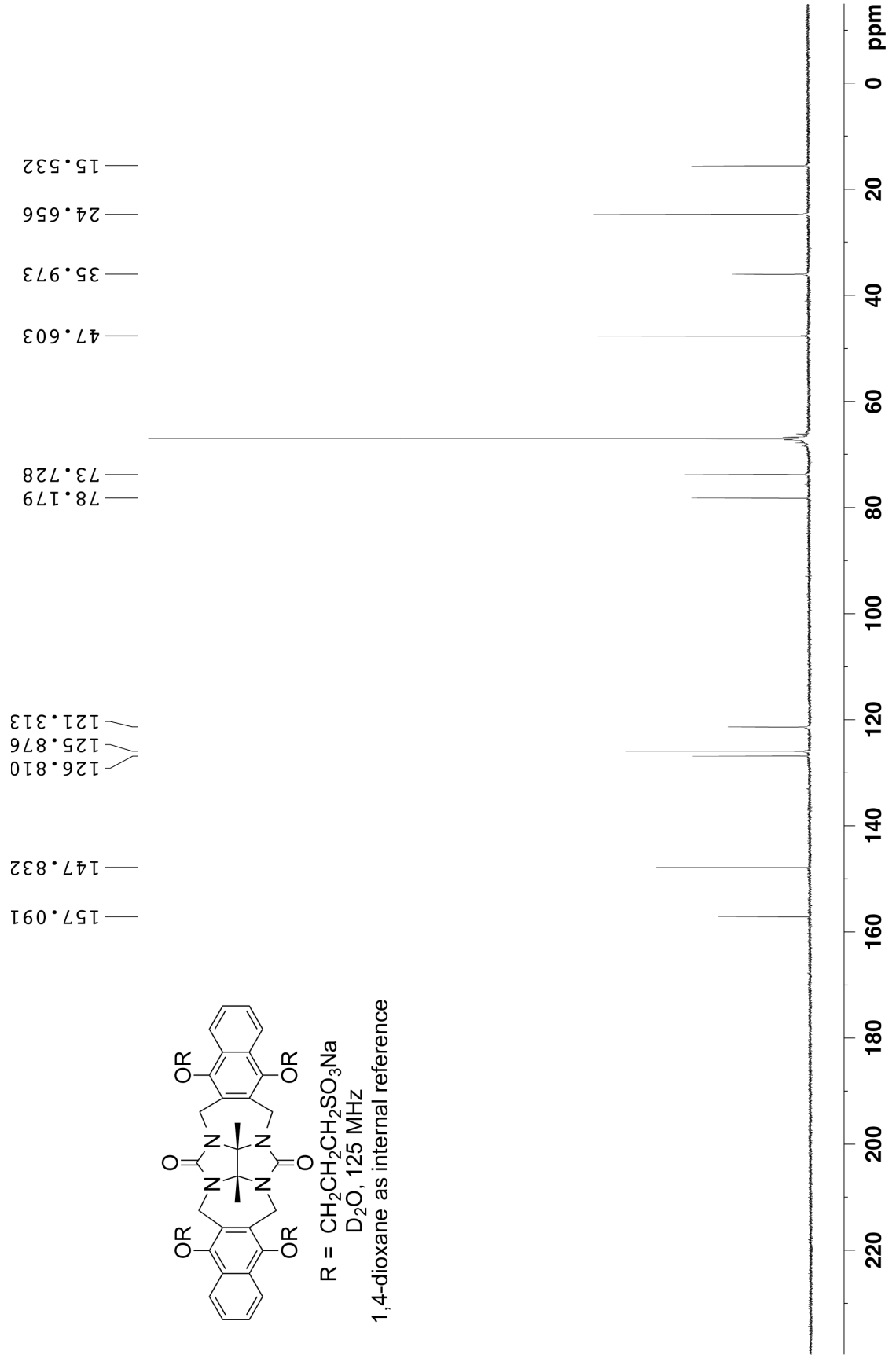

Figure S4. ^{1}H NMR recorded for compound **1b** (125 MHz, D_2O, RT, 1,4-dioxane as internal reference).

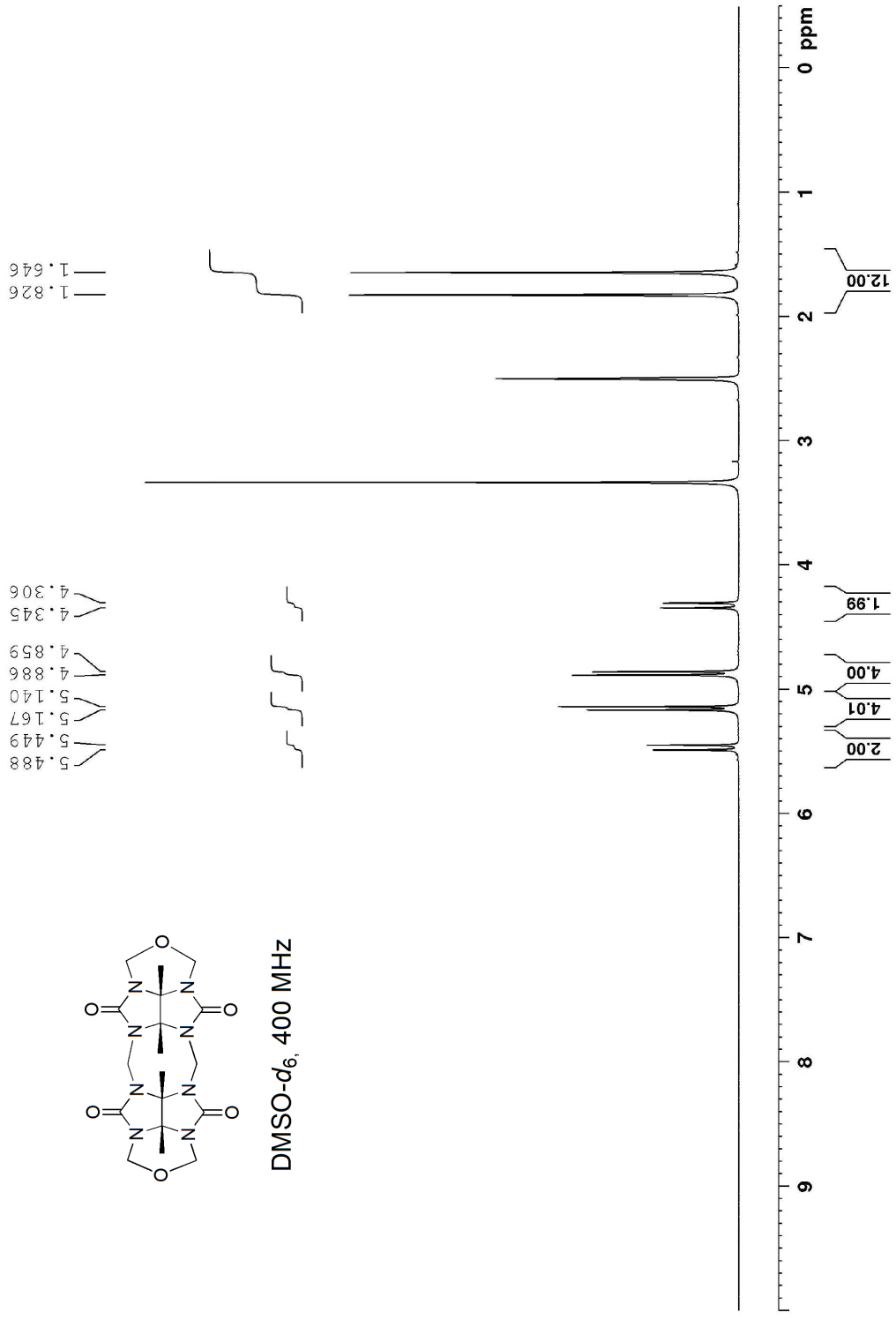

Figure S5. ^{1}H NMR recorded for compound **2CE** (400 MHz, DMSO-d_6, RT).

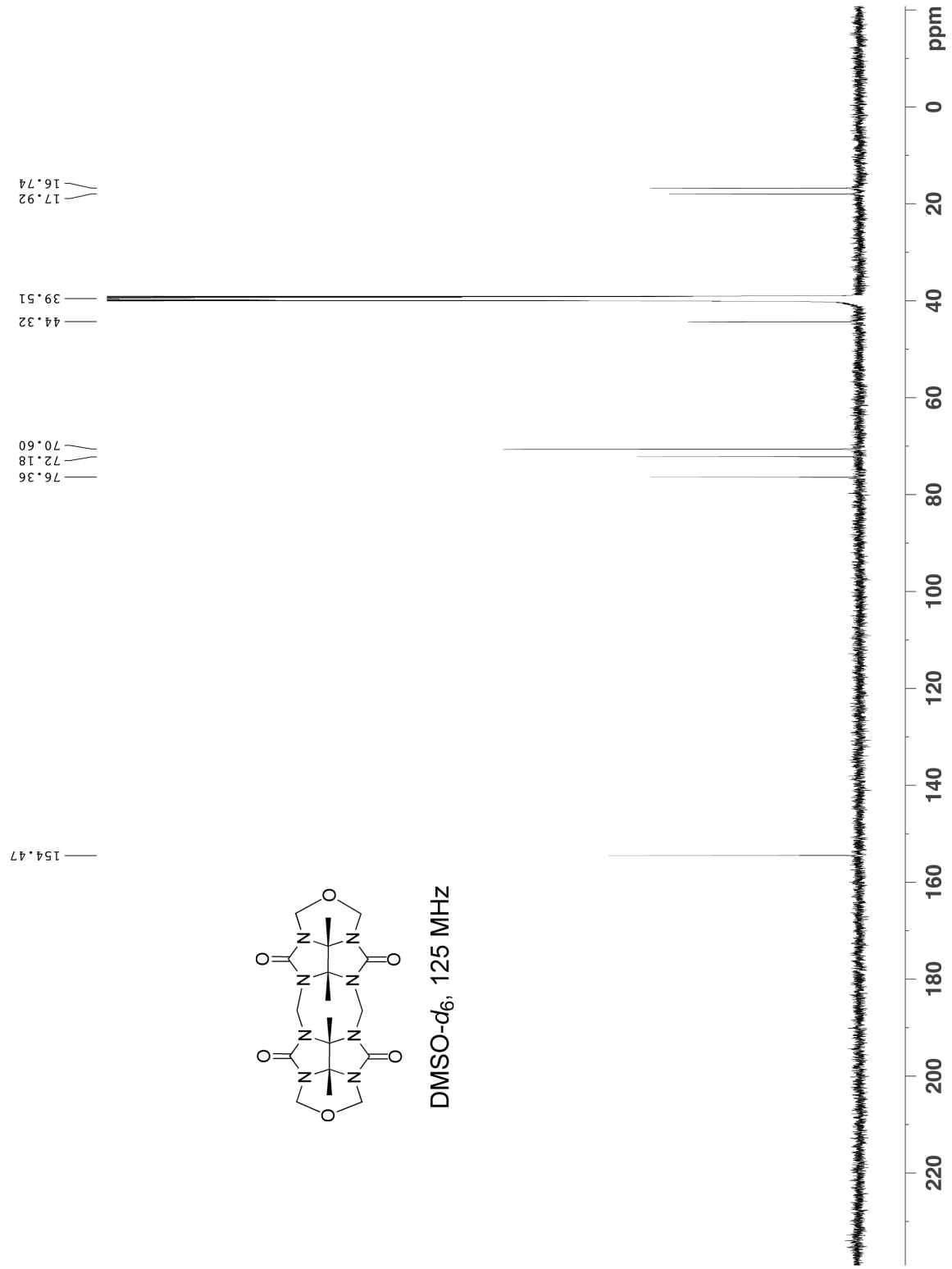

Figure S6. ^{13}C NMR recorded for compound **2CE** (125 MHz, DMSO-d_6, RT).

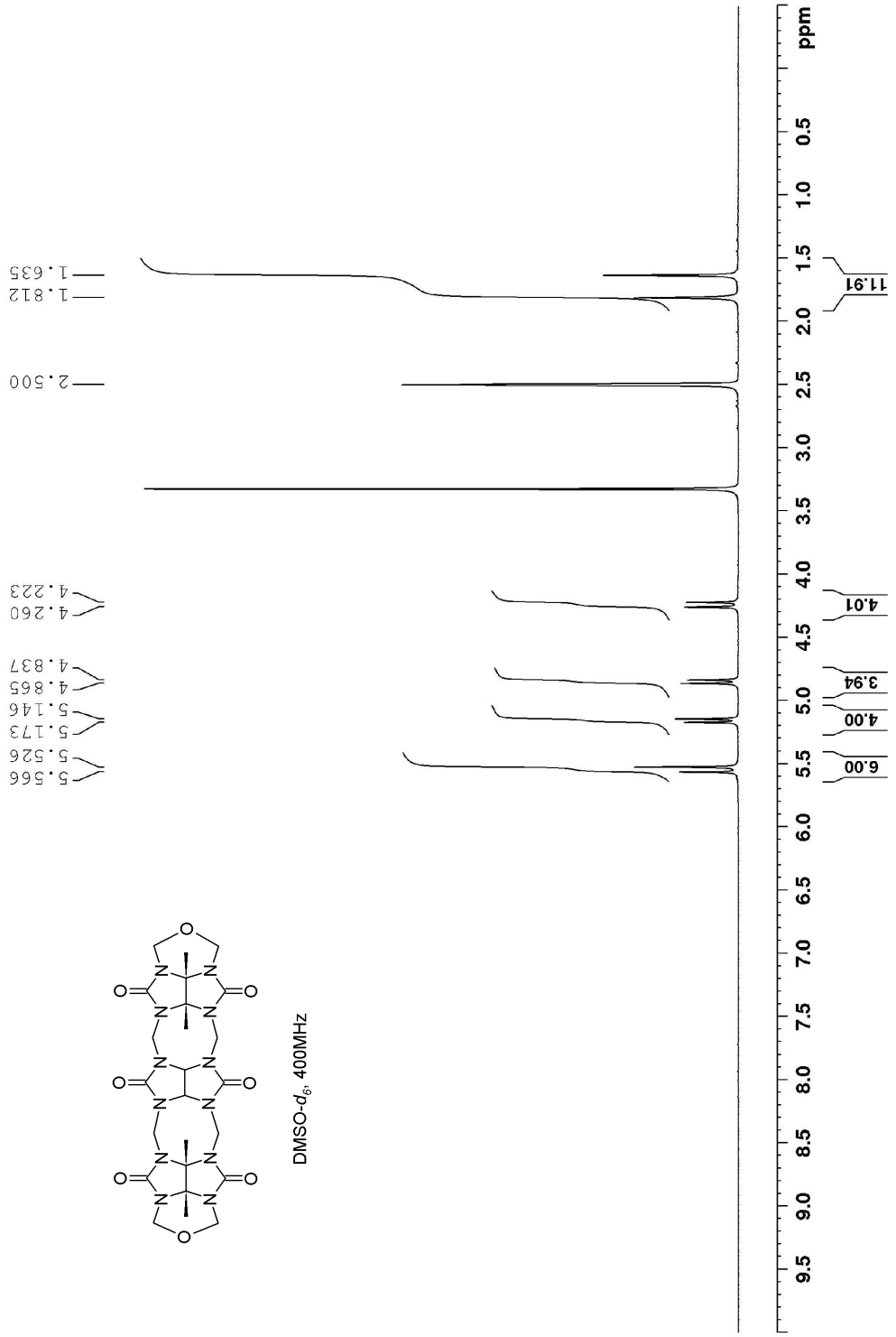

Figure S7. ^{1}H NMR recorded for compound **3CE** (400 MHz, DMSO-d_6, RT).

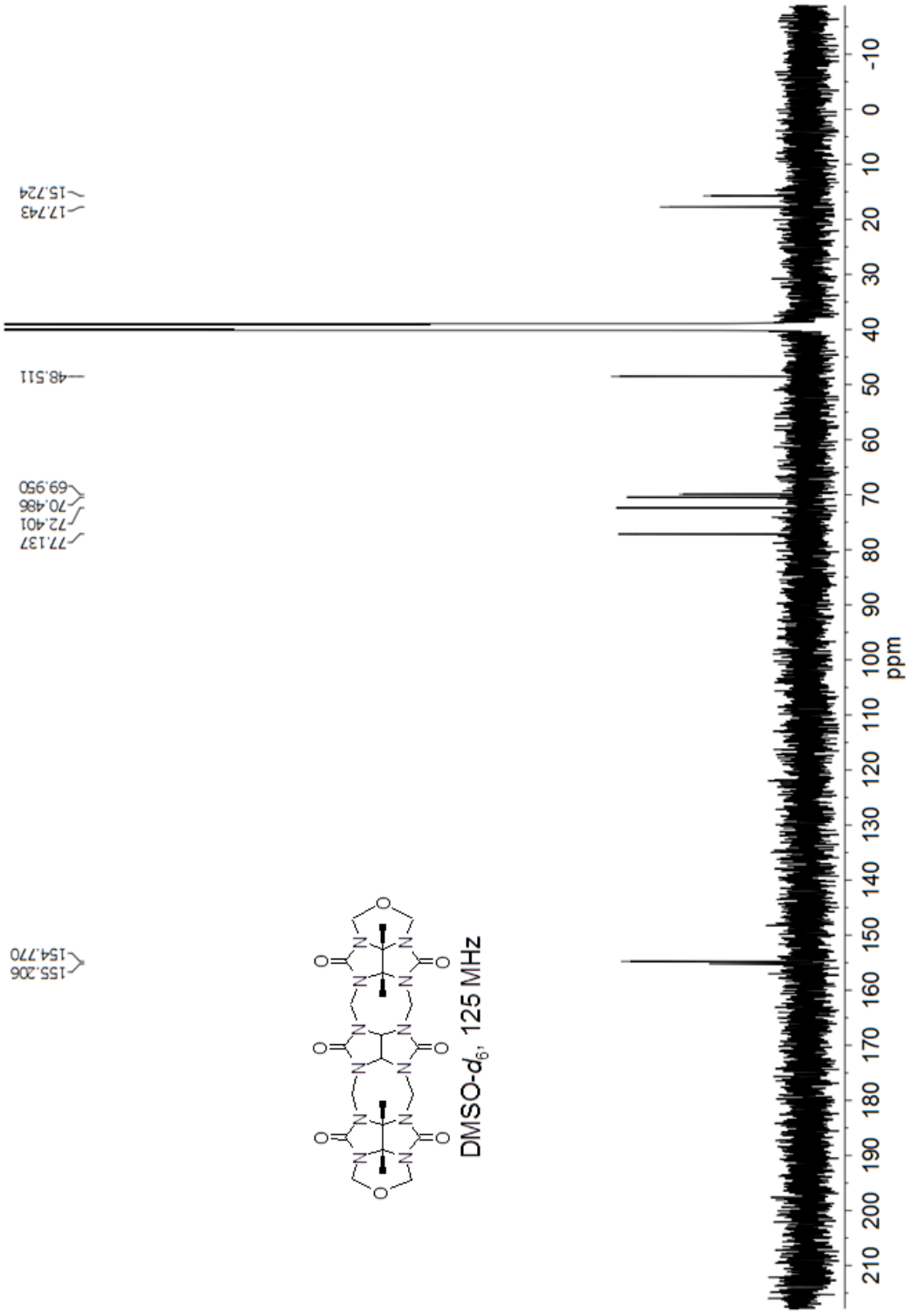

Figure S8. ^{13}C NMR recorded for compound **3CE** (125 MHz, DMSO-d_6, 30 ˚C).

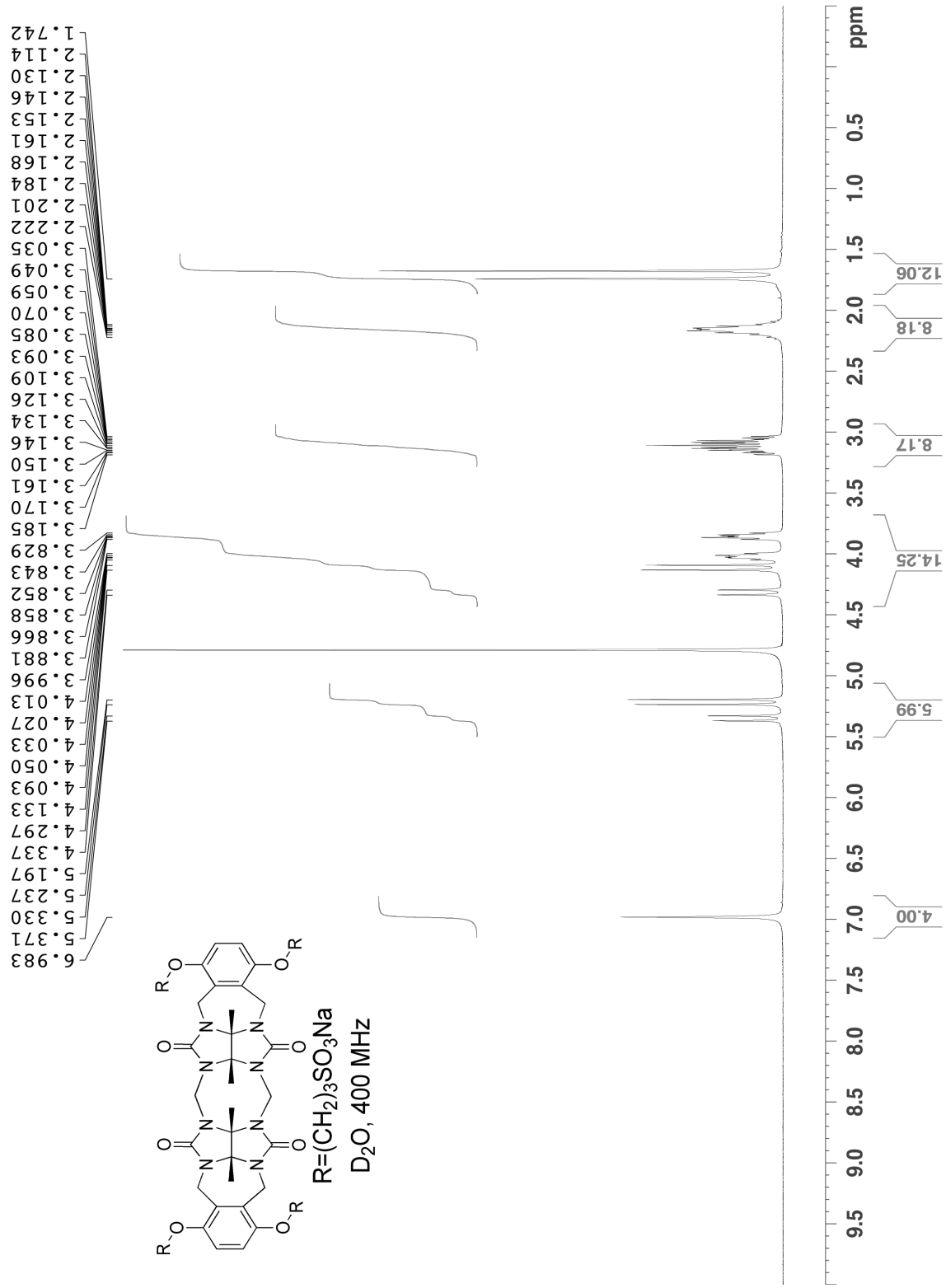

Figure S9. ^{1}H NMR recorded for compound **2a** (400 MHz, D_2O, RT).

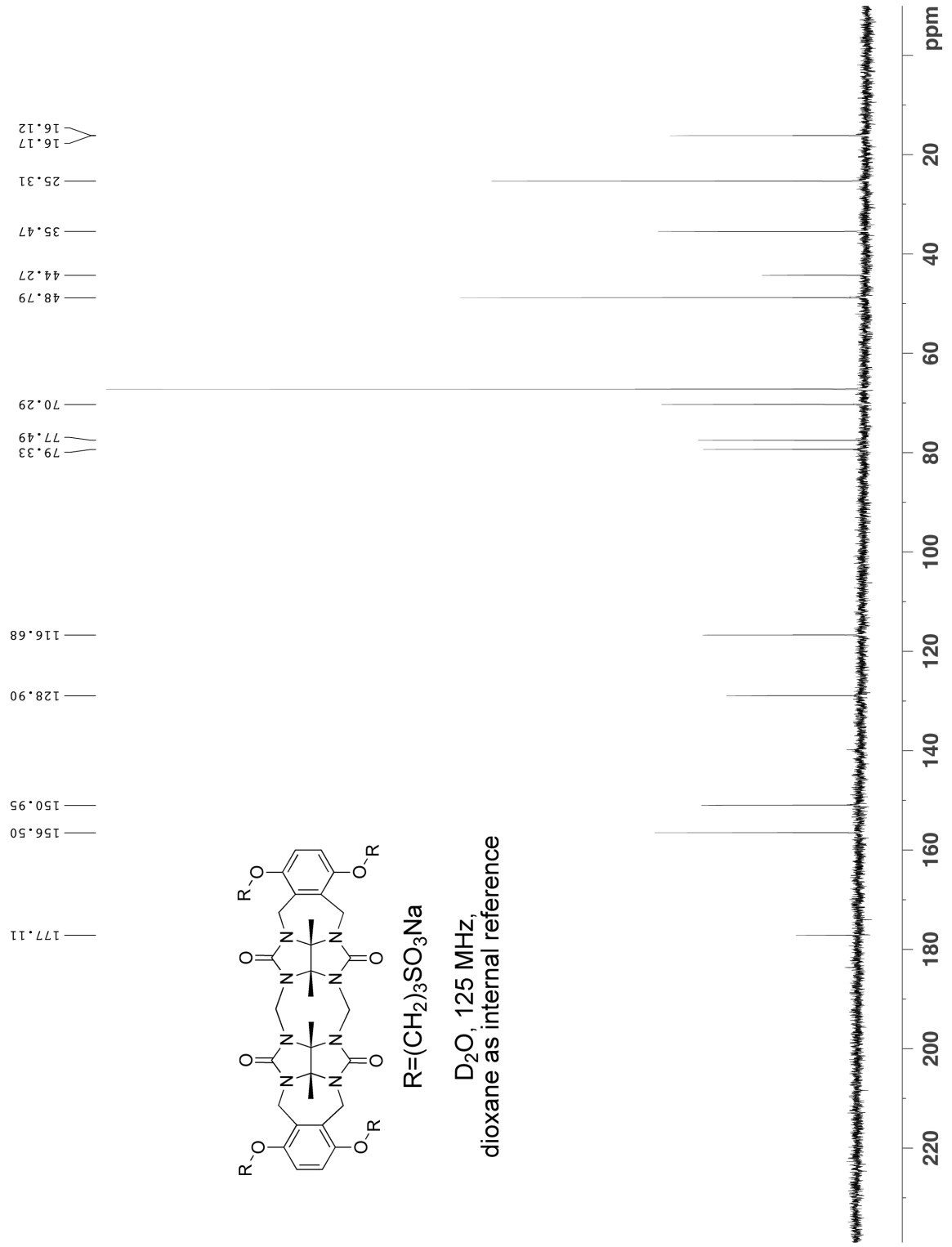

Figure S10. ^{13}C NMR recorded for compound **2a** (125 MHz, D_2O, RT, dioxane as internal reference).

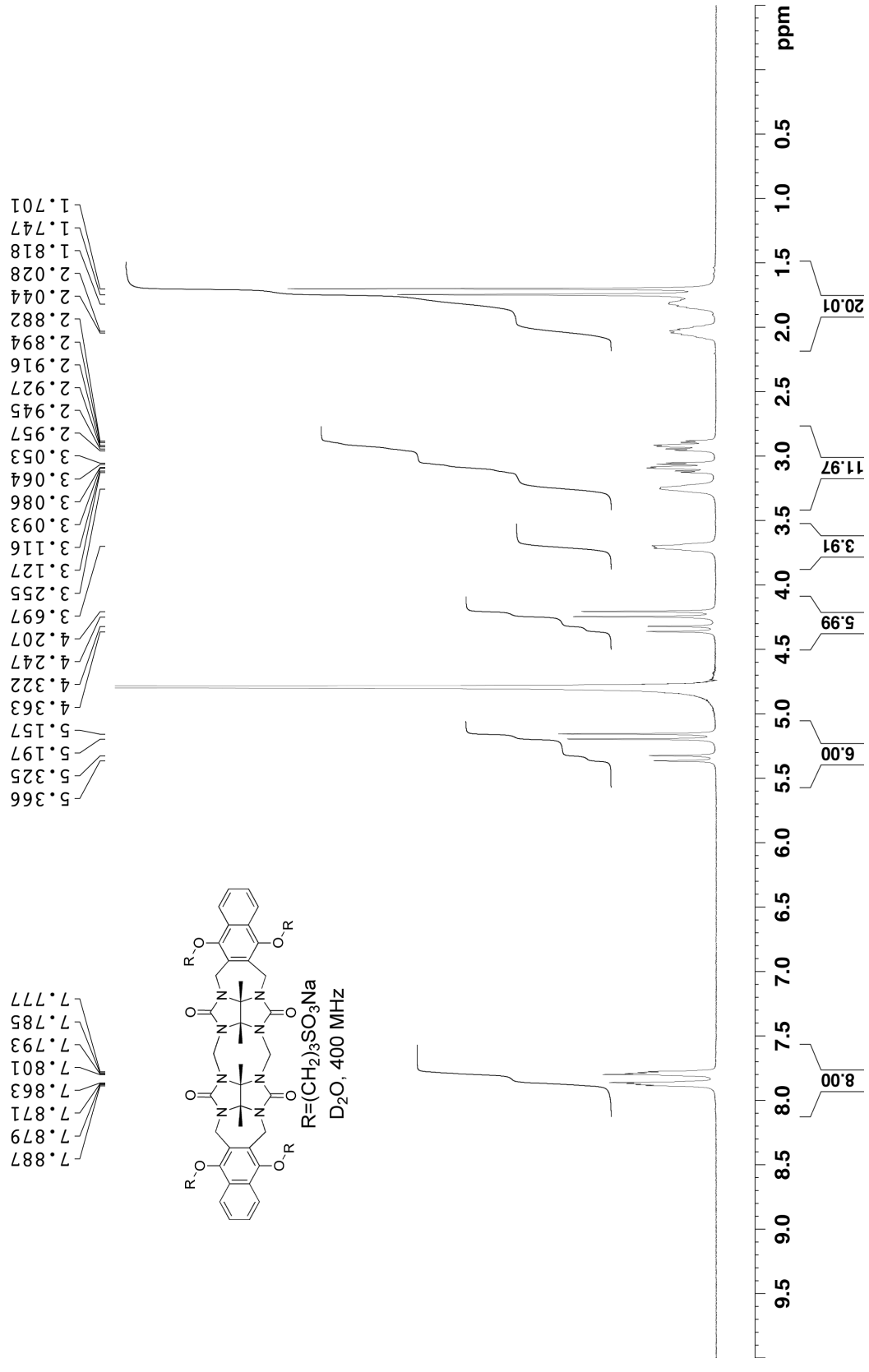

Figure S11. ^{1}H NMR recorded for **2b** (400 MHz, D_2O, RT).

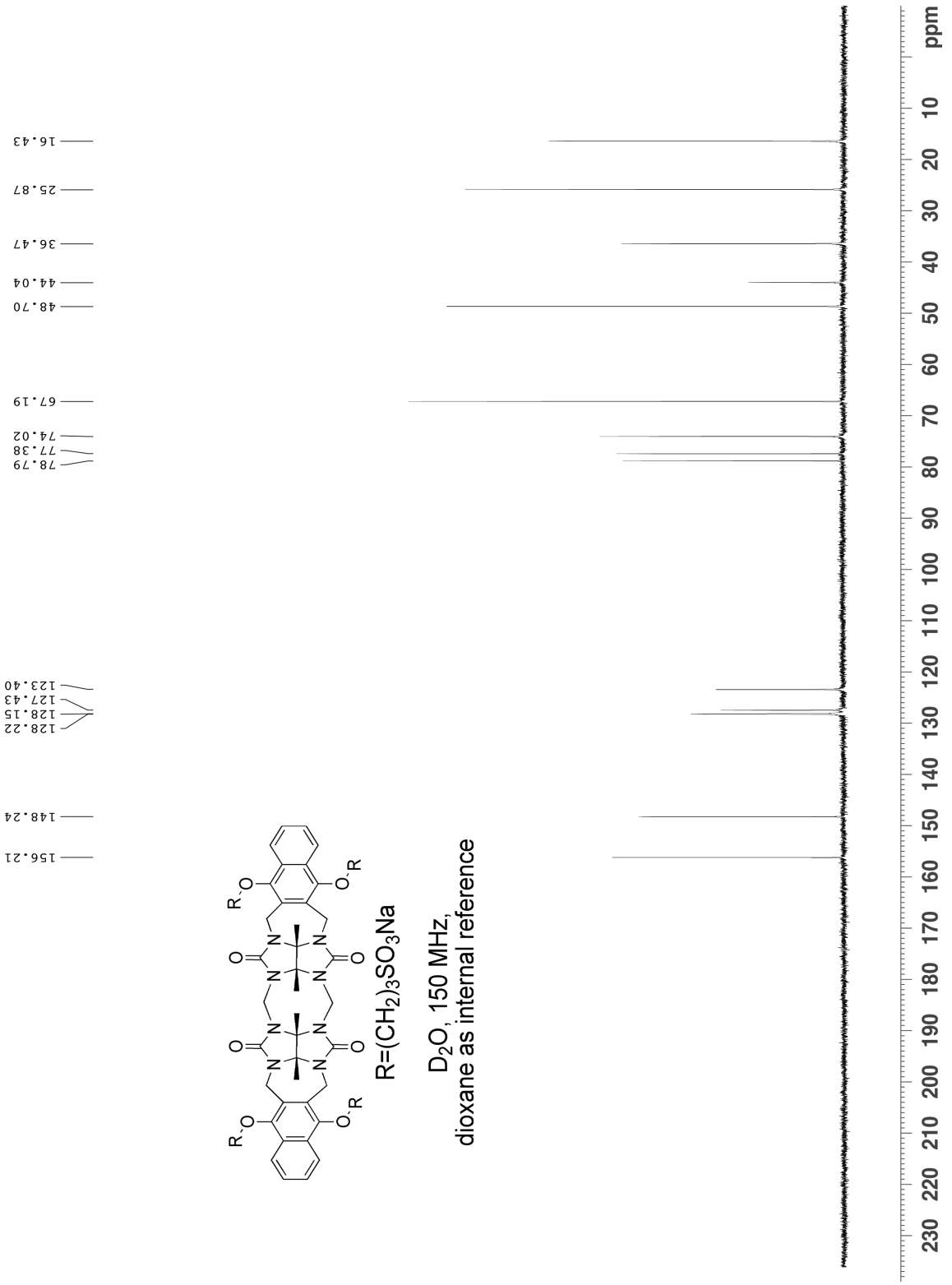

Figure S12. ^{13}C NMR recorded for compound **2b** (125 MHz, D_2O, RT, 1,4-dioxane as internal reference).

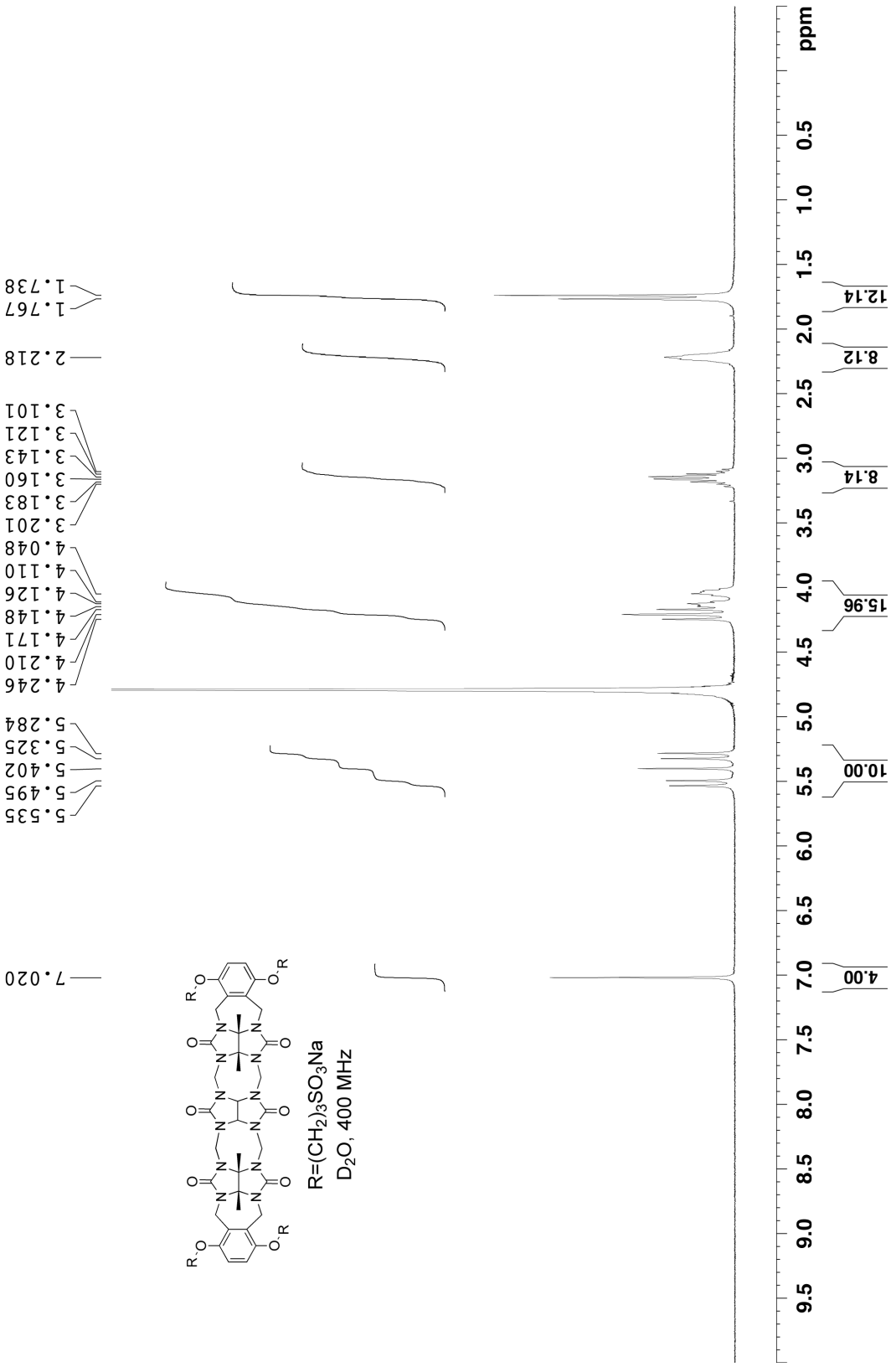

Figure S13. ^{1}H NMR recorded for compound **3a** (400 MHz, D_2O, RT).

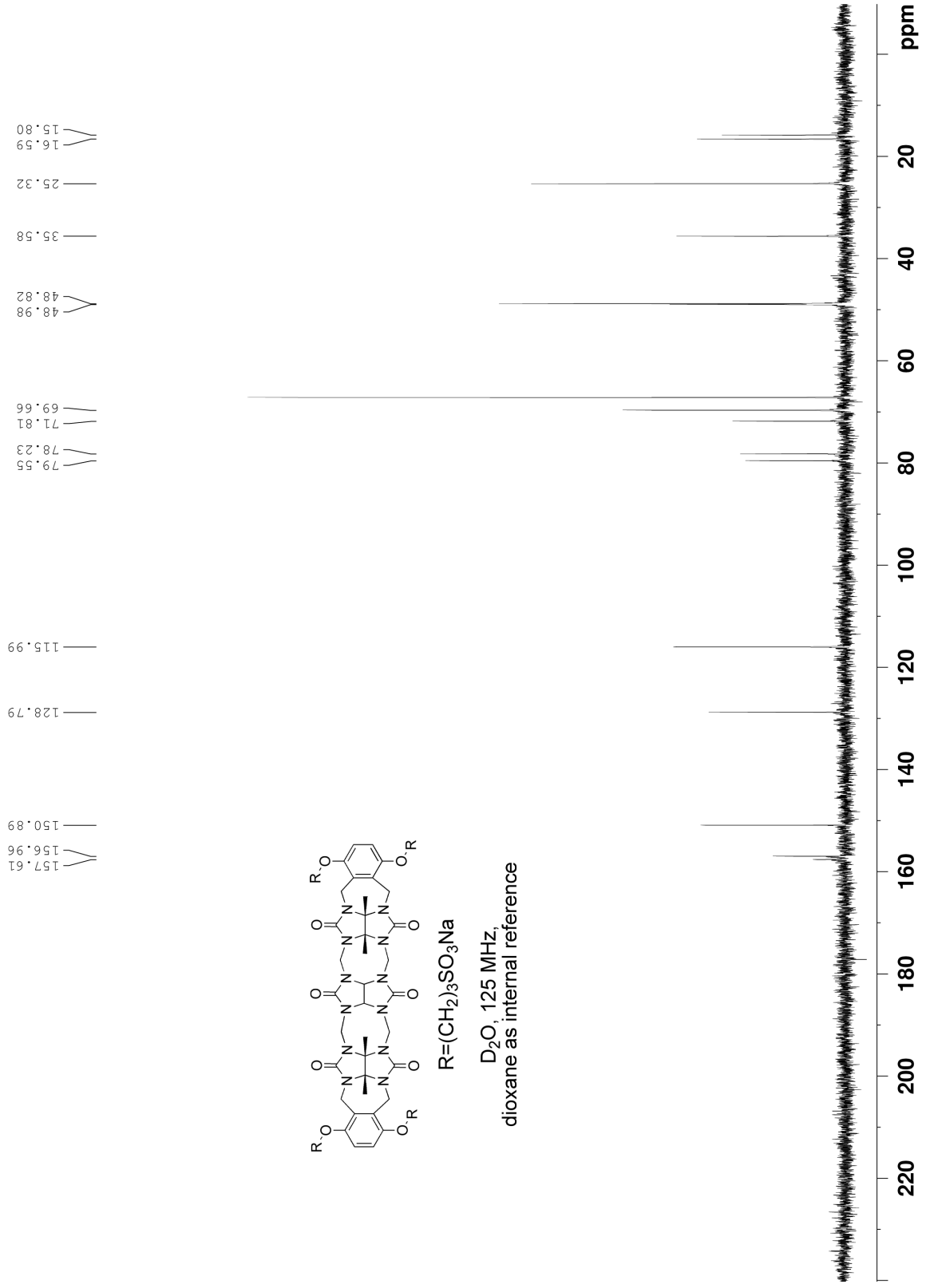

Figure S14. ^{13}C NMR recorded for compound **3a** (125 MHz, D_2O, RT, dioxane as internal reference).

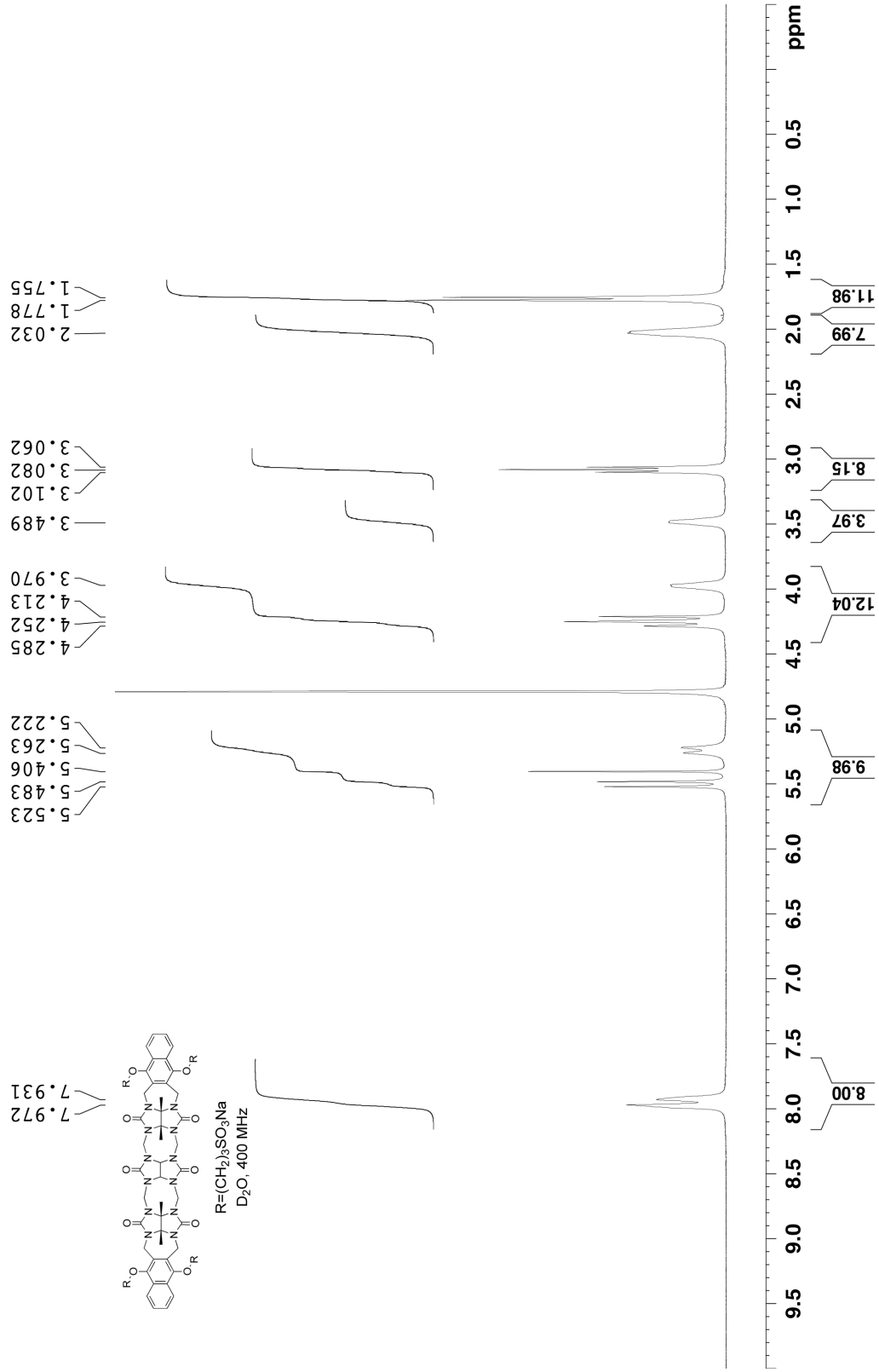

Figure S15. ^{1}H NMR recorded for compound **3b** (400 MHz, D_2O, RT).

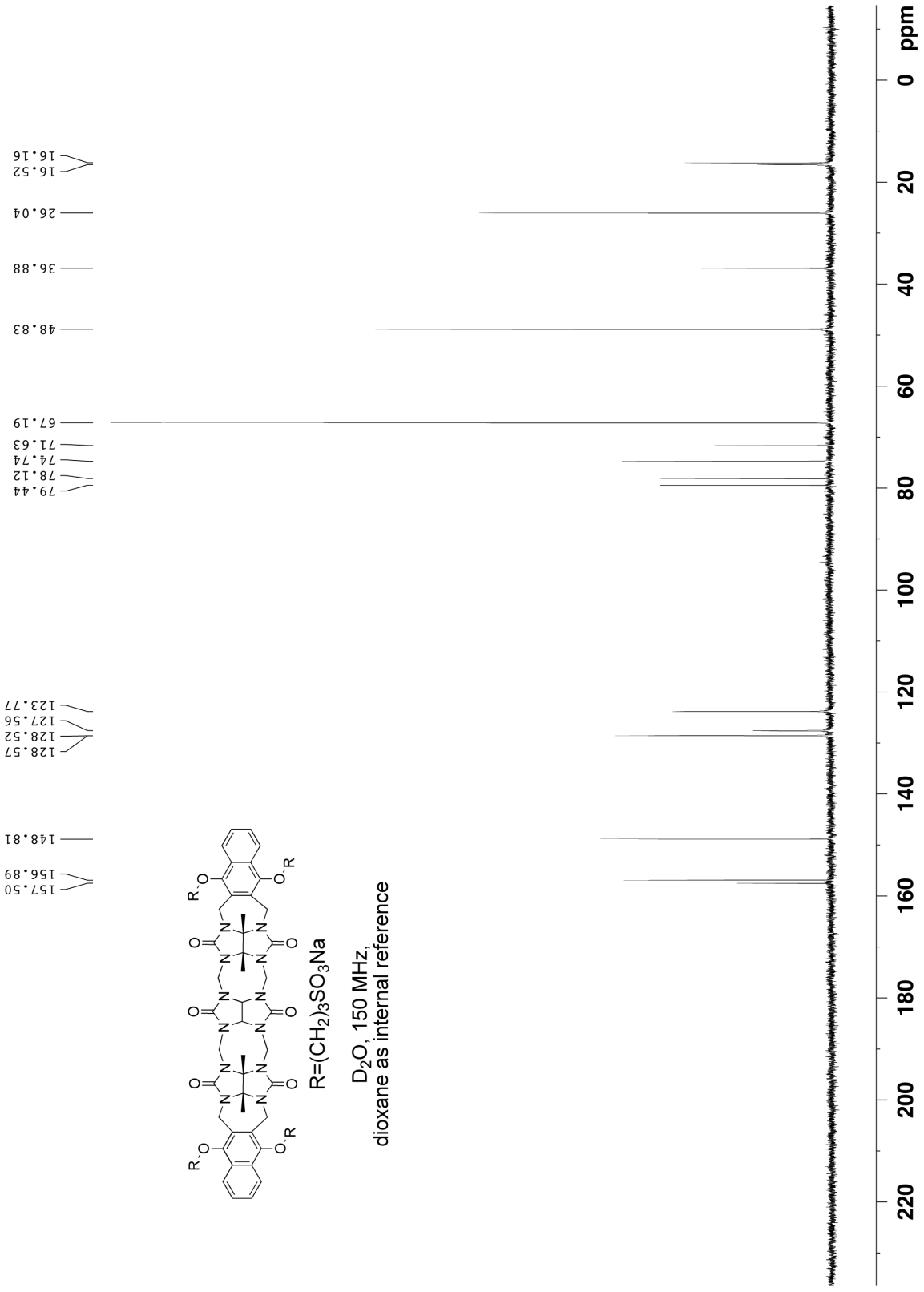

Figure S16. ^{13}C NMR recorded for compound **3b** (150 MHz, D_2O, RT, dioxane as internal reference).

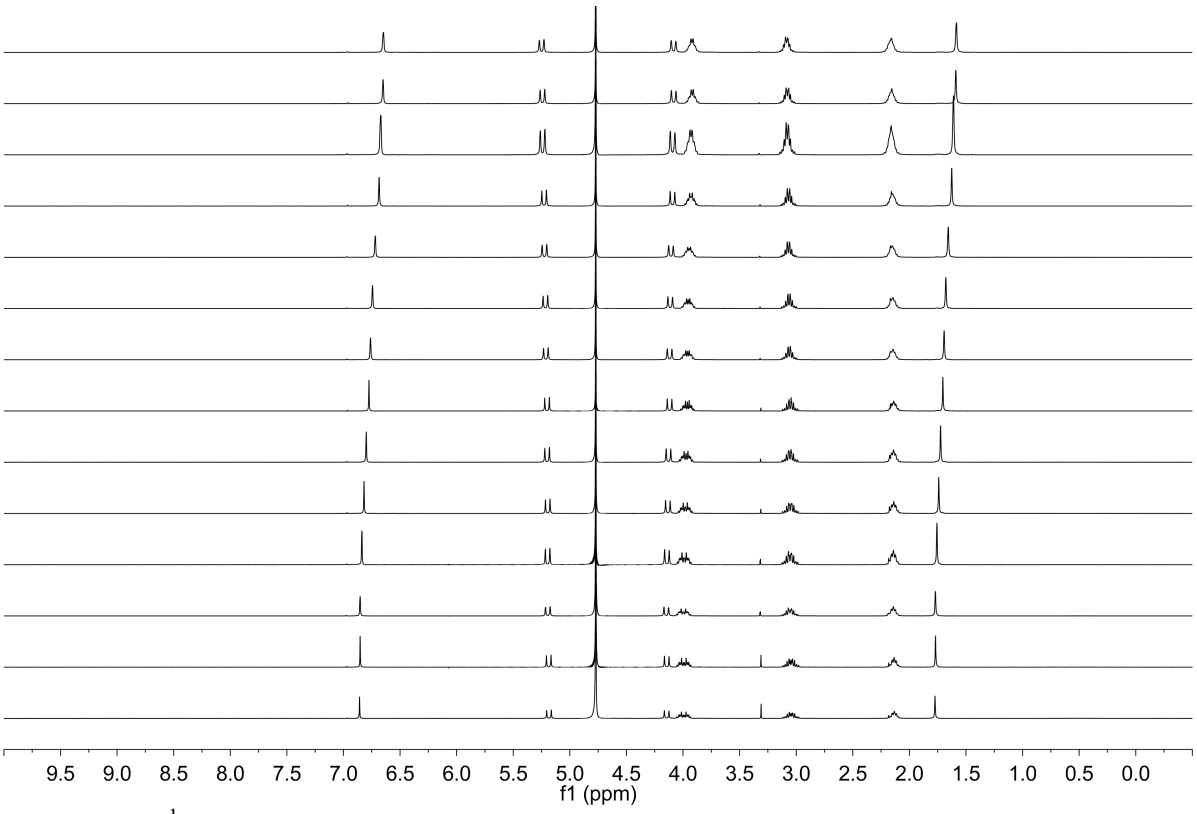

Figure S17. ^{1}H NMR recorded for **1a** at varied concentration 0.1 mM – 50 mM **(**400 MHz, 20 mM NaD2PO4, pD = 7.4) for self-association study.

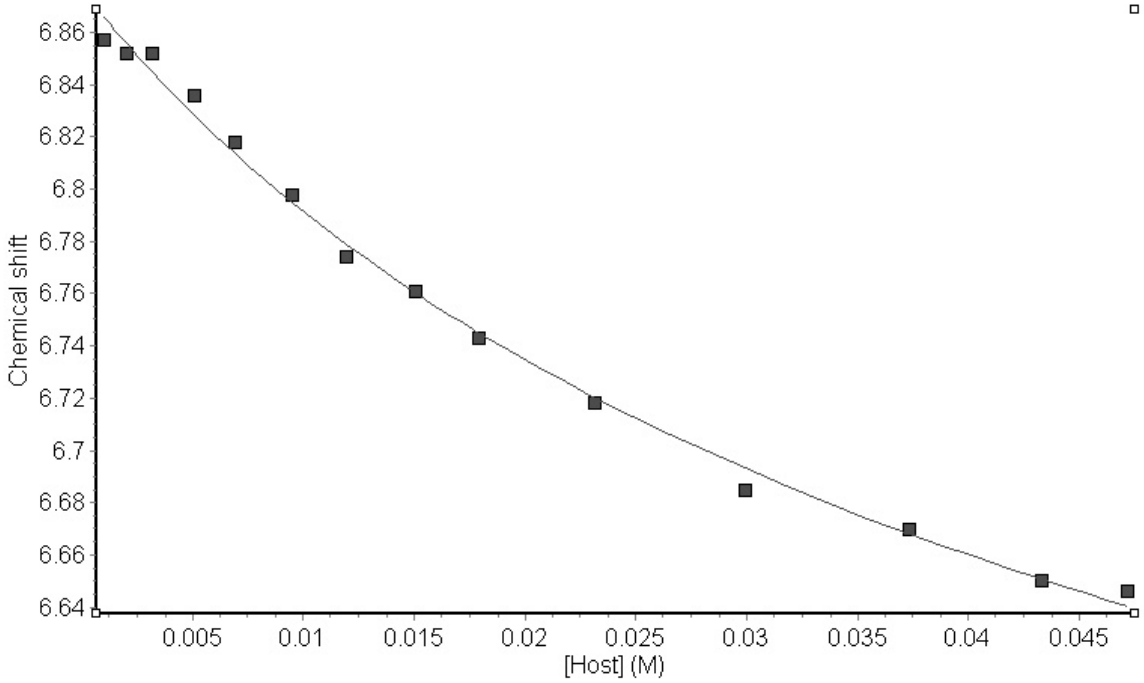

Figure S18. Plot of chemical shift of **1a** versus [**1a**]. The solid line represents the best non-linear fitting of the data to a two-fold self-association model with K_s = 30 M^{-1}.

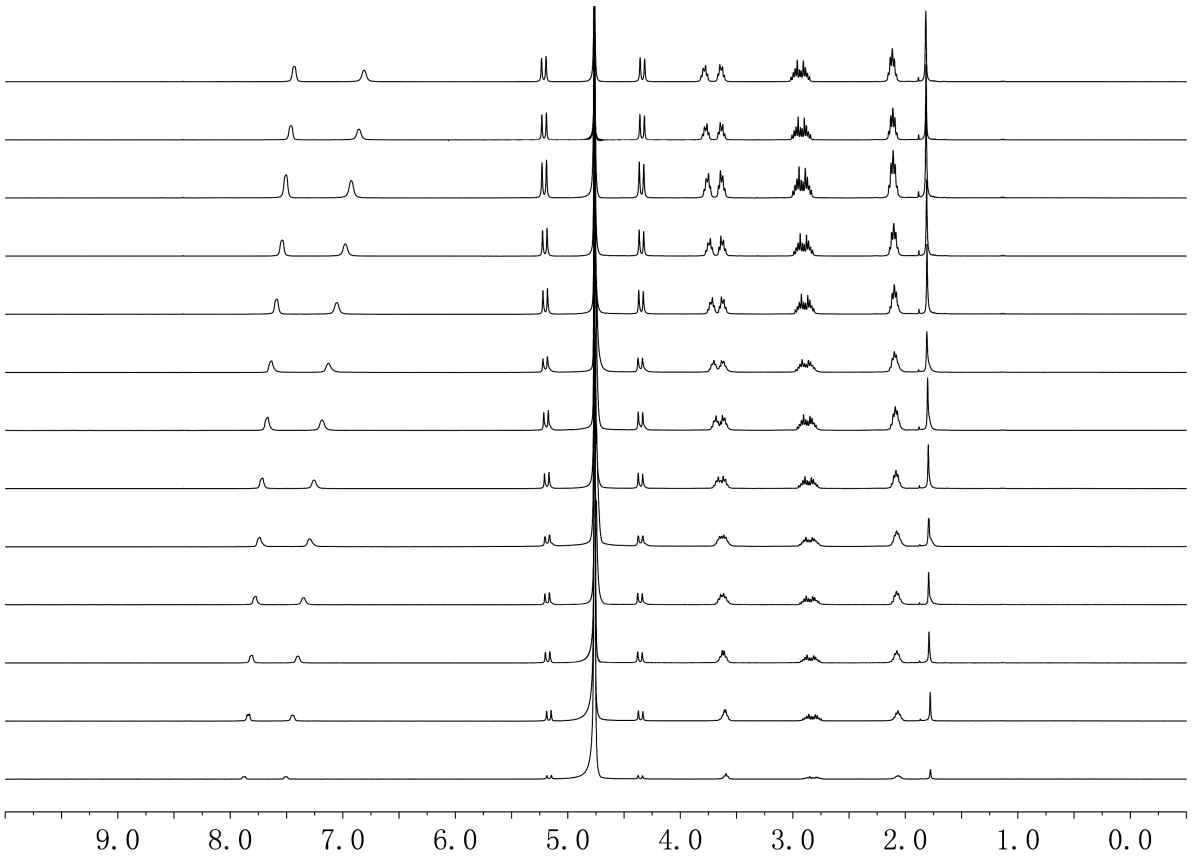

Figure S19. ^{1}H NMR recorded (400 MHz, 20 mM NaD2PO4, pD = 7.4) for **1b** at different concentrations (0.1 mM – 20 mM) for self-association study.

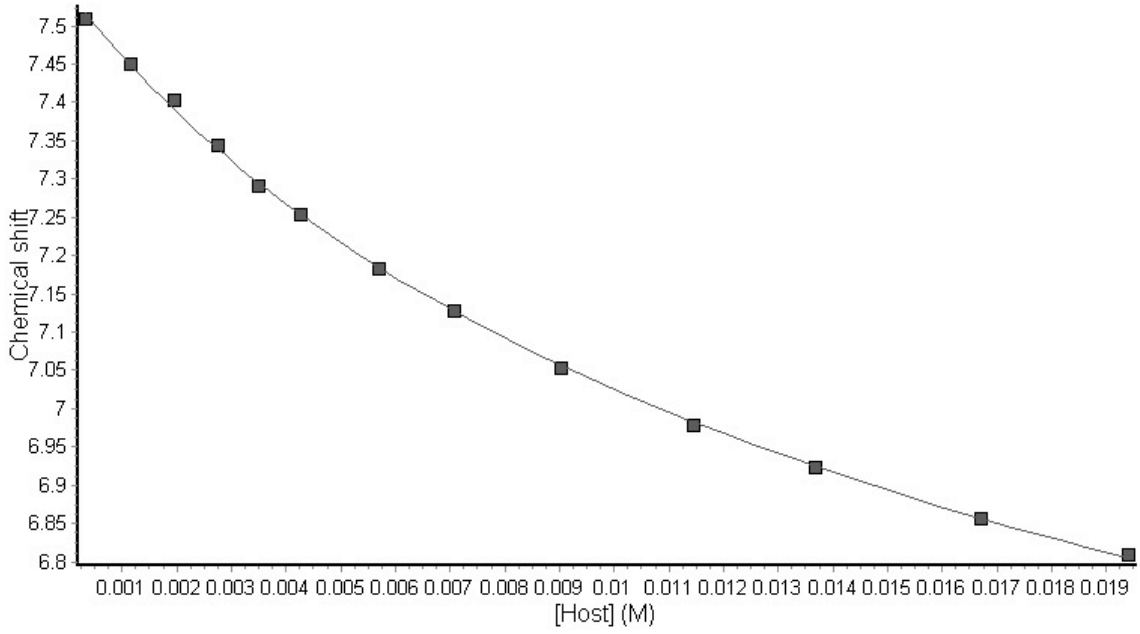

Figure S20. Plot of chemical shift of **1b** versus [**1b**]. The solid line represents the best non-linear fitting of the data to a two-fold self-association model with K_s = 92 M^{-1}.

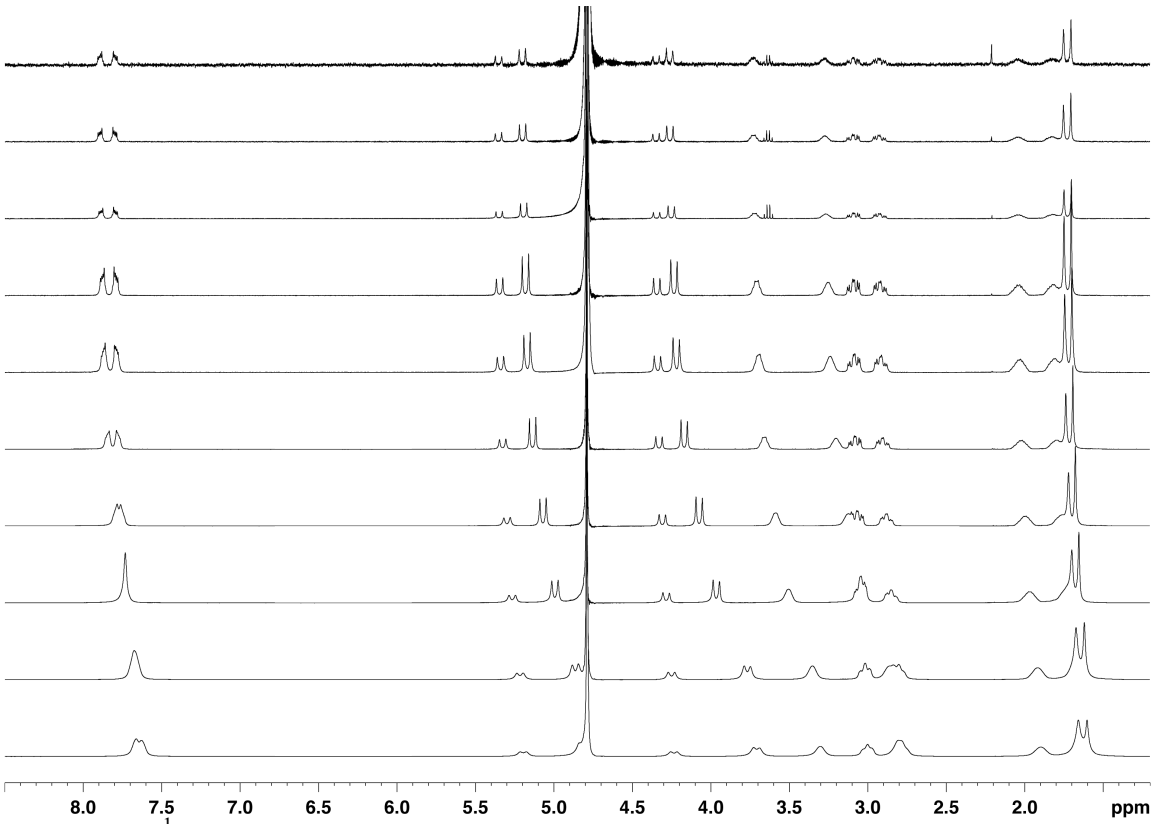

Figure S21 ^{1}H NMR recorded for **2b** at different concentrations (0.1 mM to 190 mM) (400 MHz, 20 mM NaD_2PO_4, pD = 7.4) for self-association study.

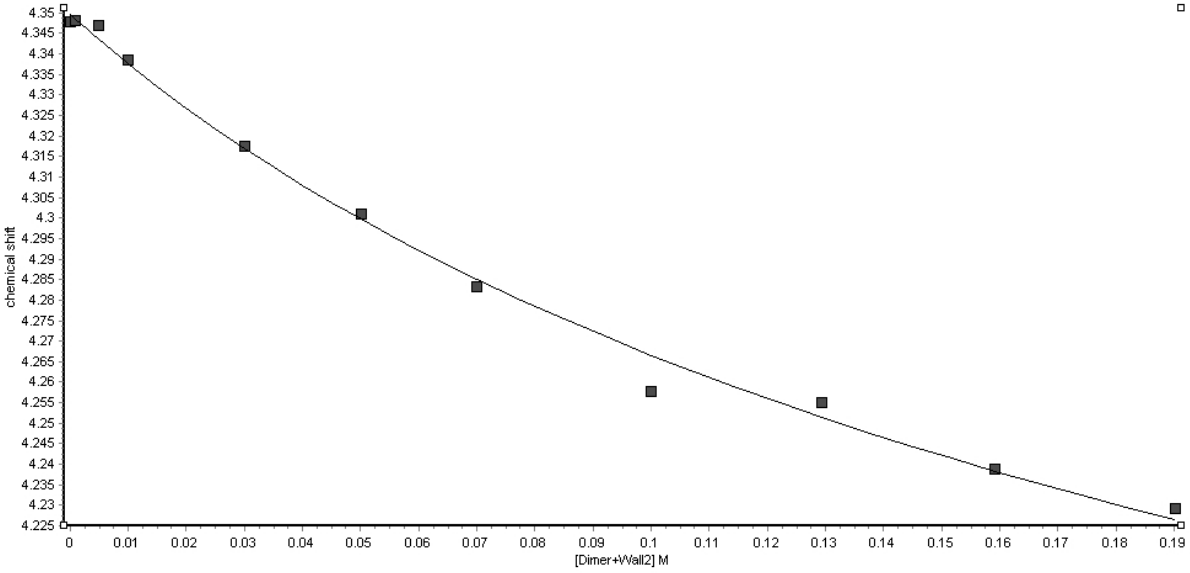

Figure S22. Plot of chemical shift of **2b** versus [**2b**] The solid line represents the best non-linear fitting of the data to a two-fold self-assocation model with K_s = 6 M^{-1}.

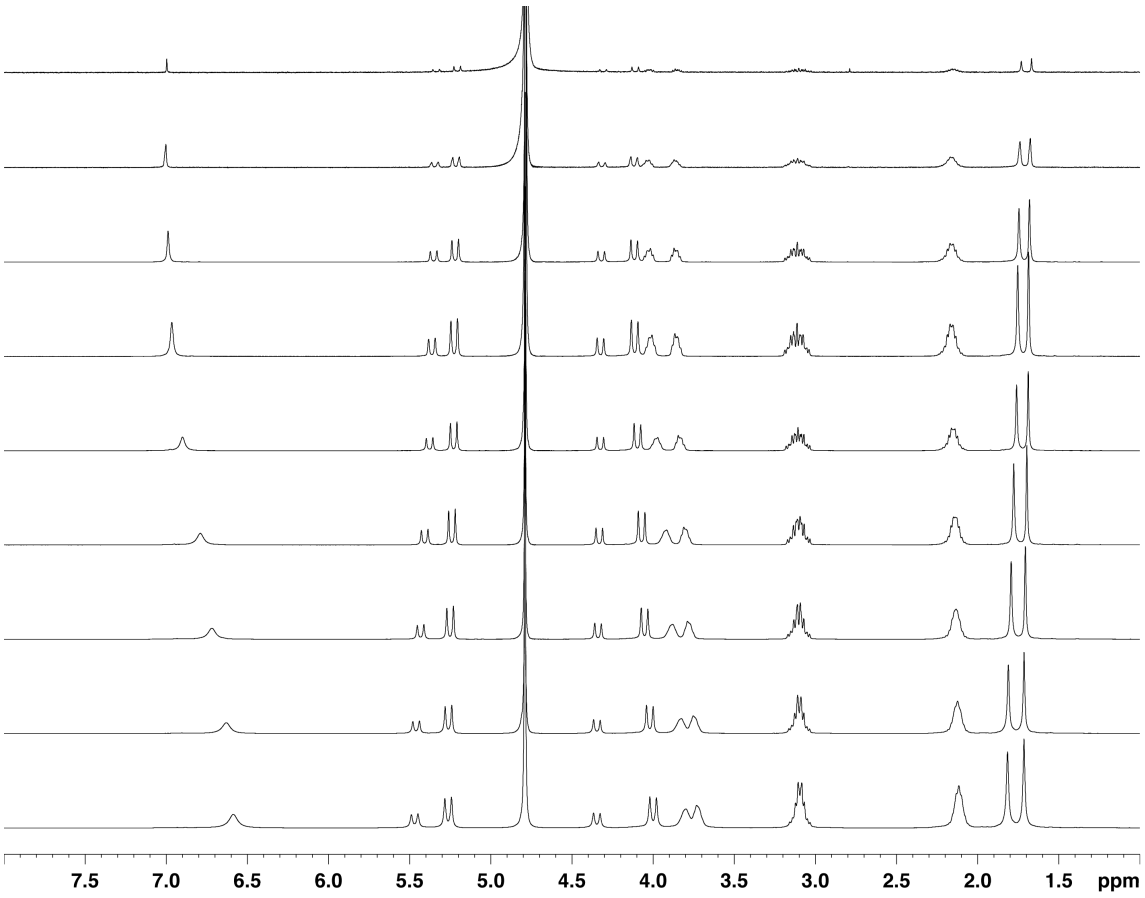

Figure S23. ^{1}H NMR recorded for **2a** at varied concentration 0.1 mM to 156 mM **(**400 MHz, 20 mM NaD2PO4, pD = 7.4) for self-association study.

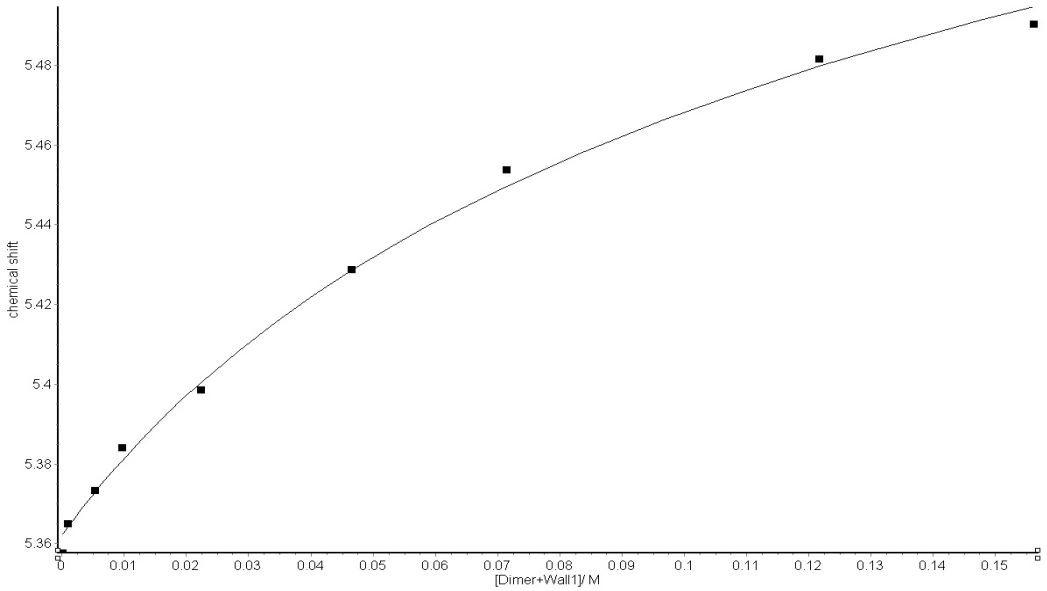

Figure S24. Plot of chemical shift of **2a** versus [**2a**]. The solid line represents the best non-linear fitting of the data to a two-fold self-assocation model with K_s = 12 M^{-1}.

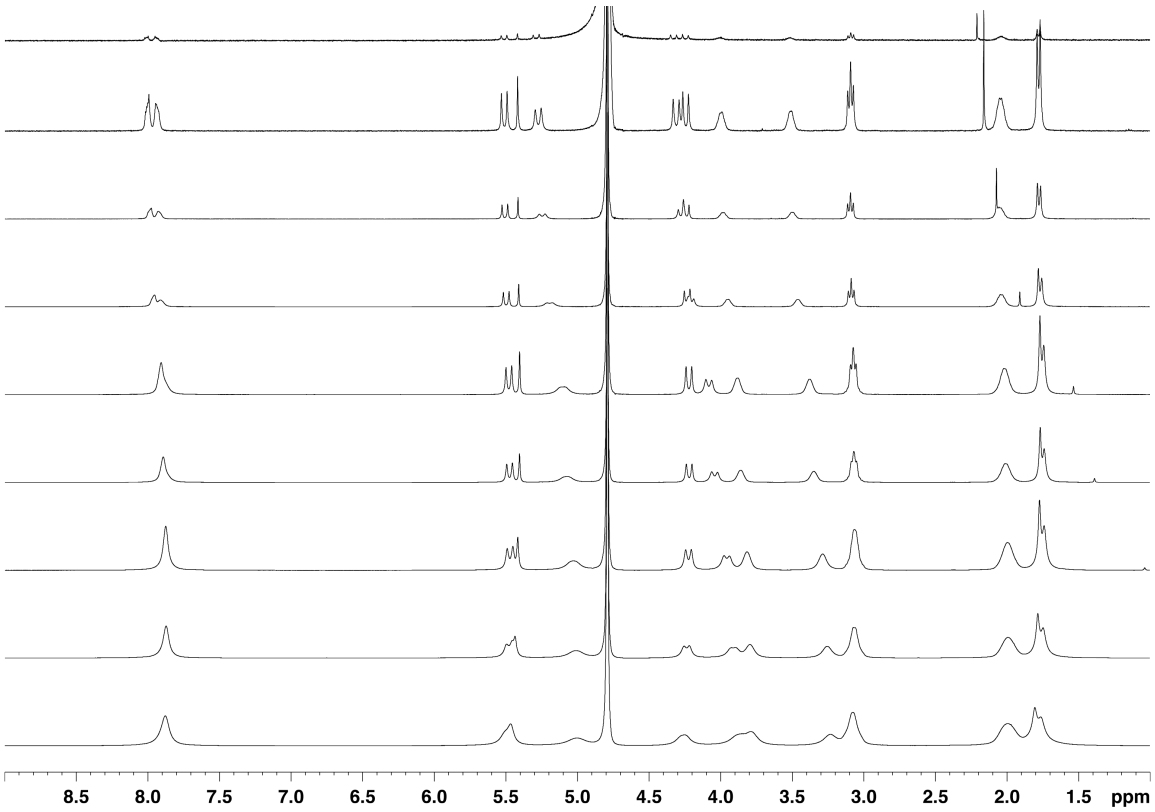

Figure S25. ^{1}H NMR recorded (400 MHz, 20 mM NaD2PO4, pD = 7.4) for **3b** at different concentrations (0.1 mM to 137 mM) for self-association study.

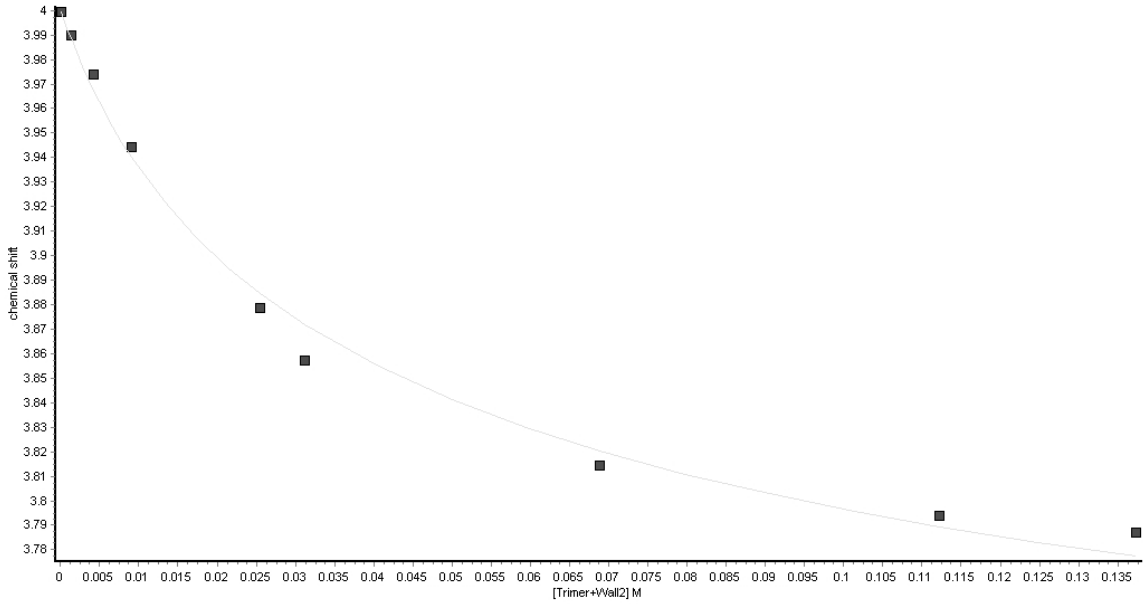

Figure S26. Plot of chemical shift of **3b** versus [**3b**]. The solid line represents the best non-linear fitting of the data to a two-fold self-association model with K_s = 49 M^{-1}.

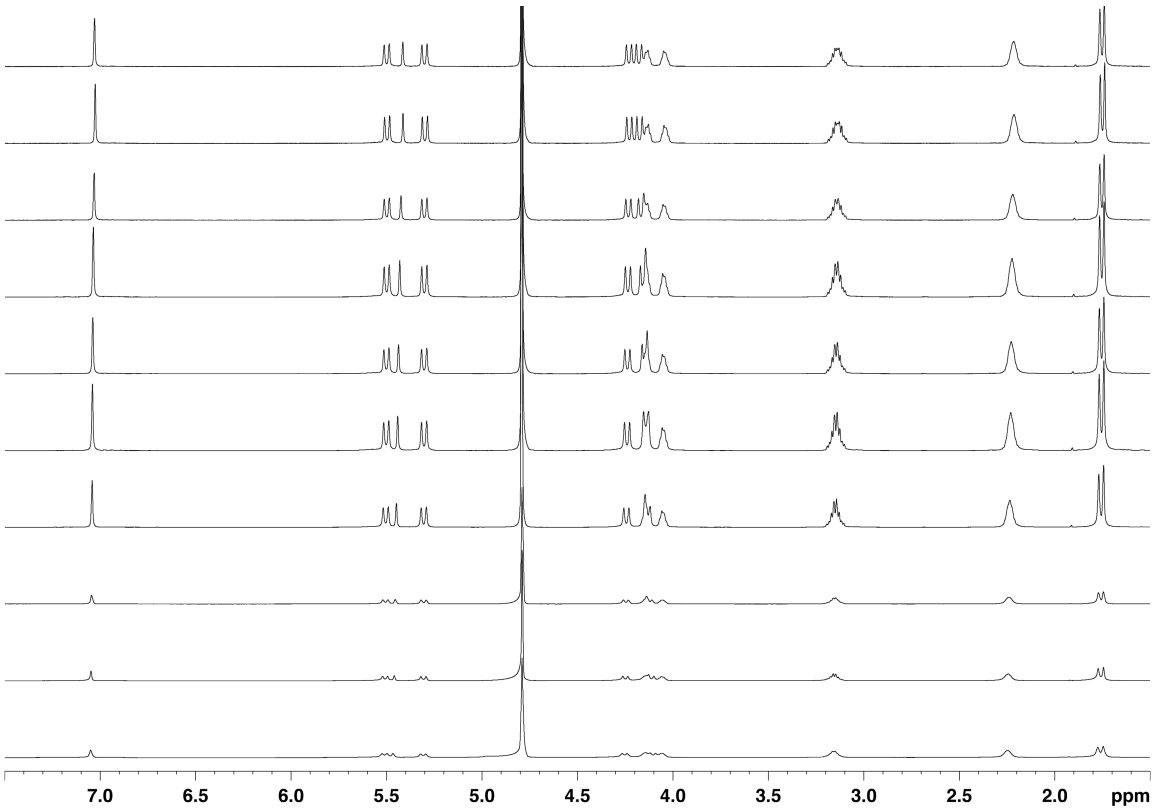

Figure S27. ^{1}H NMR recorded for **3a** at varied concentration 0.1 mM to 102 mM **(**400 MHz, 20 mM NaD2PO4, pD = 7.4) for self-association study.

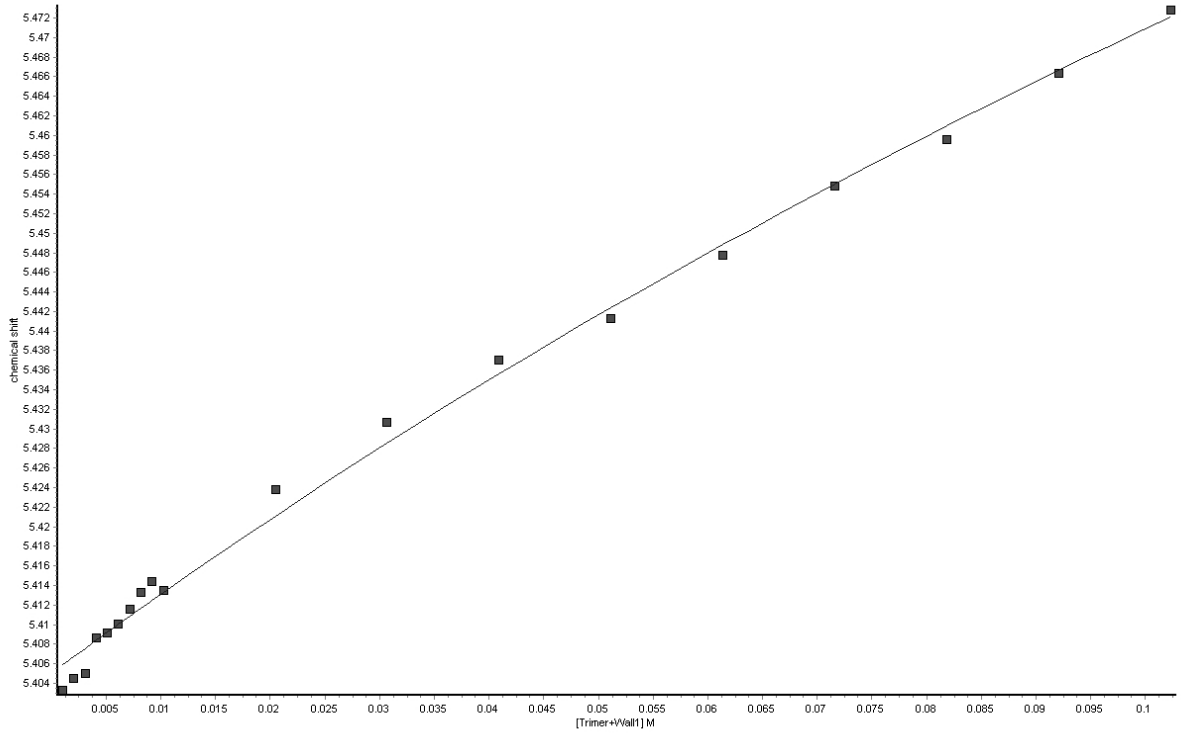

Figure S28. Plot of chemical shift of **3a** versus [**3a**]. The solid line represents the best non-linear fitting of the data to a two-fold self-assocation model with K_s = 3 M^{-1}.

Procedure to measure the solubility of containers 1-3. Excess amount of container was stirred in deuterated sodium phosphate buffer (20 mM, pD = 7.4). The suspended mixture was magnetically stirred at room temperature for 12 h. During this period, the pD value of the solution was monitored and adjusted back to 7.4 if it changed. The mixture was then filtered and diluted (usually 10-fold). The ^{1}H NMR spectrum of the supernatant was measured (400 MHz) after addition of 1,3,5-benzenetricarboxylic acid (usually 1.00 mM) as internal standard. The signal for the internal standard resonates at 8.35 ppm (s, 3H). Diagnostic signals for the containers were also integrated. From the ratio of the integrals of the internal standard relative to the drug resonances, and the concentration of reference, the concentration of the containers can be calculated.

Procedure to measure the solubility of drugs with Host 1 – 3. Excess amount of drug was added into a solution of host (**1 – 3**) of known concentration in deuterated sodium phosphate buffer (20 mM, pD = 7.4). The suspended mixture was magnetically stirred at room temperature for 6 h. During this period, the pD value of the solution was monitored and adjusted back to 7.4 if it changed. The mixture was then filtered. The ^{1}H NMR spectrum of the supernatant was measured (400 MHz) with 1,3,5-benzenetricarboxylic acid (1.00 mM) as internal standard. The resonance for the internal standard appears at 8.35 ppm (s, 3H). Diagnostic signals for the dissolved drug were also integrated. From the ratio of integrals of the internal standard relative to the resonances for the drug, and the known concentration of internal standard allows calculation of the concentration of the drug.

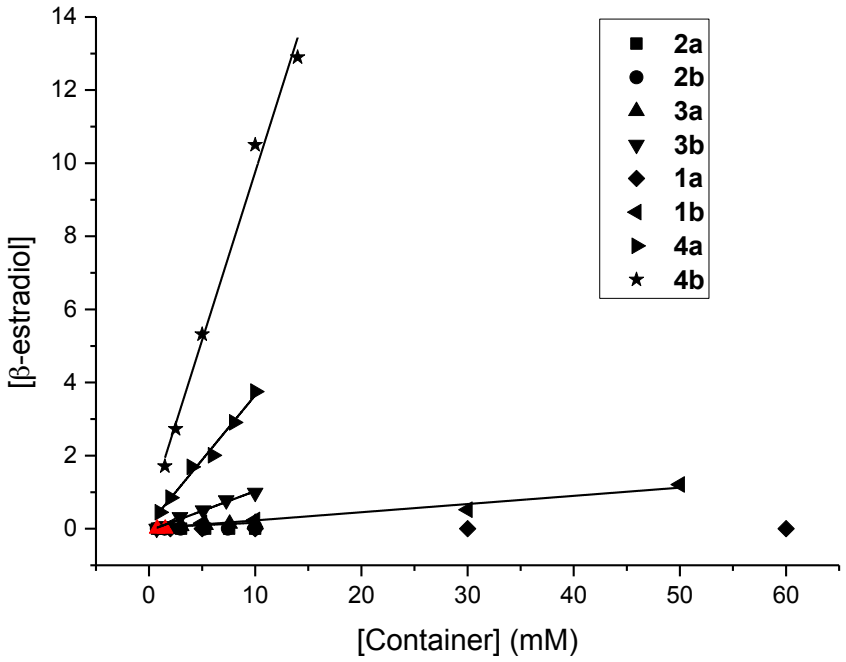

Figure S29. Phase solubility diagram of β-estradiol with different hosts in sodium phosphate buffer (20 mM, pH 7.4, RT). Data points shown in red were not used in the linear fit.

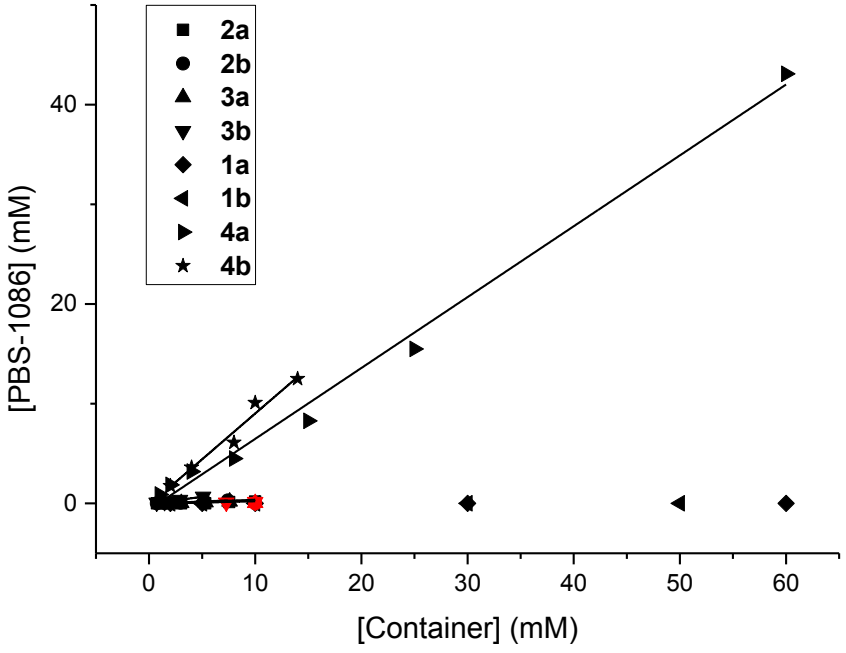

Figure S30. Phase solubility diagram of PBS-1086 with different hosts in sodium phosphate buffer (20 mM, pH 7.4, RT). Data points shown in red were not used in the linear fit.

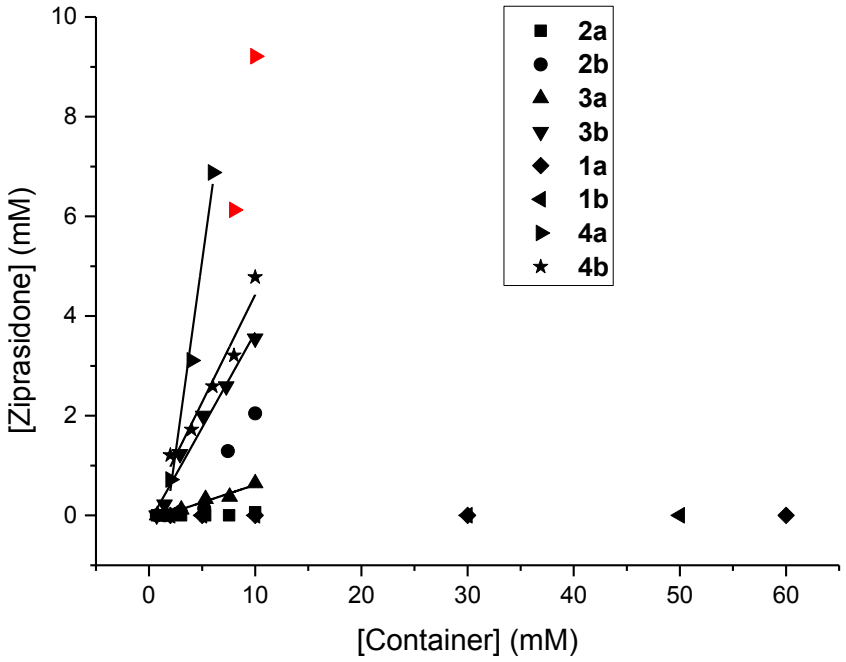

Figure S31. Phase solubility diagram of ziprasidone with different hosts in sodium phosphate buffer (20 mM, pH 7.4, RT). Data points shown in red were not used in the linear fit.

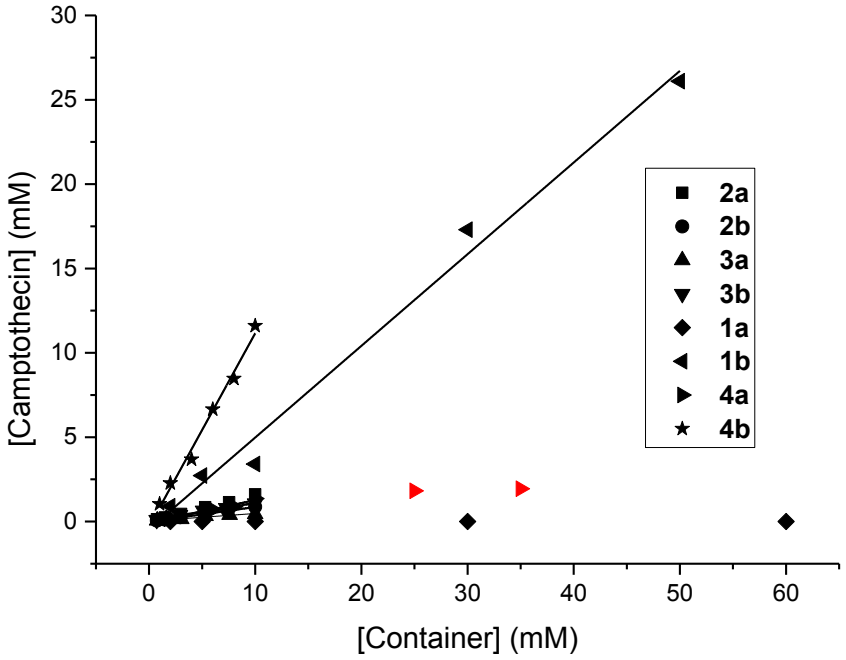

Figure S32. Phase solubility diagram of Camptothecin with different hosts in sodium phosphate buffer (20 mM, pH 7.4, RT). Data points shown in red were not used in the linear fit.

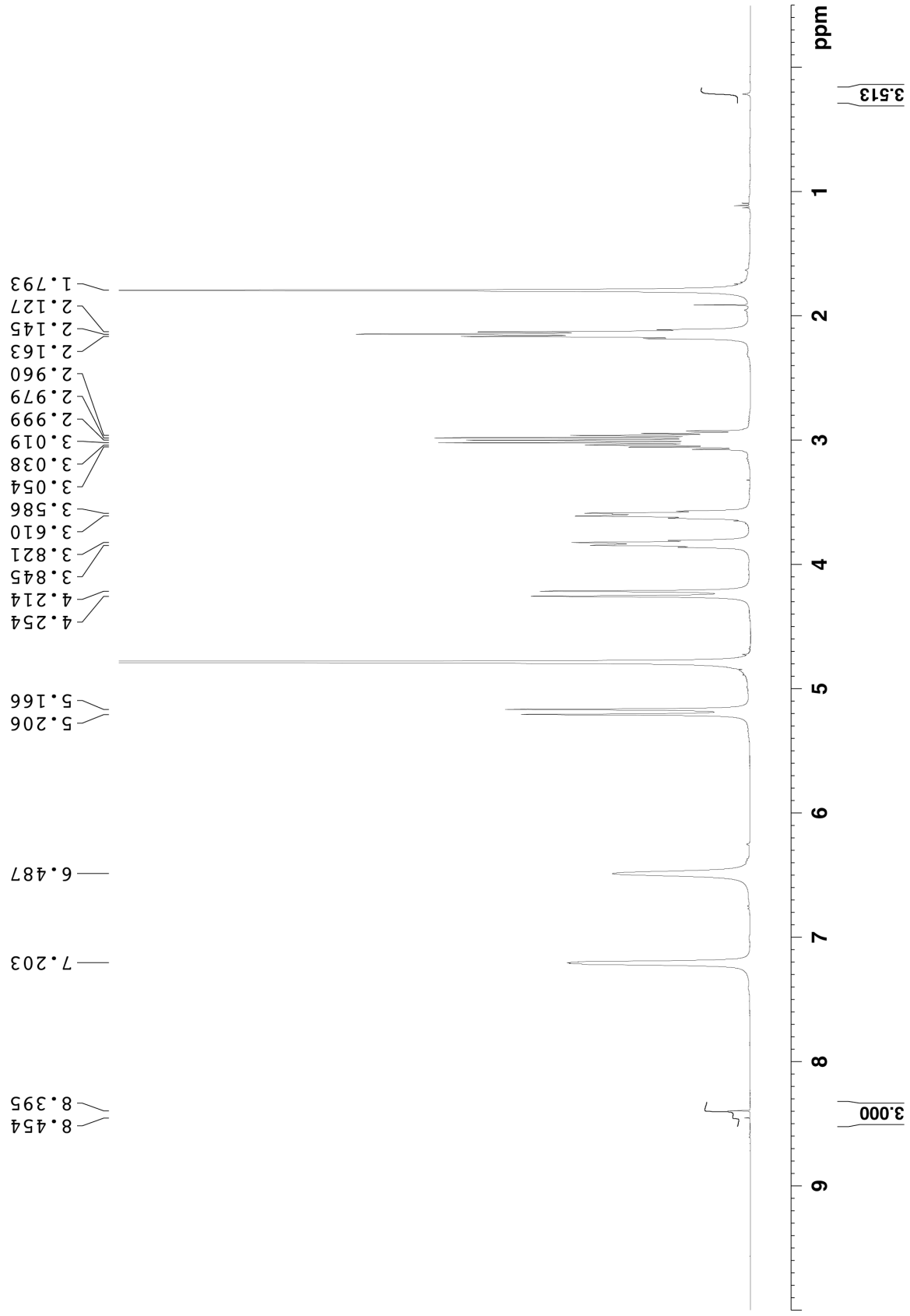

Figure S33. ^{1}H NMR recorded for estradiol with **1b** (50 mM) (400 MHz, 20 mM NaD_2PO_4, pD 7.4, RT, 1,3,5 benzenetricarboxylic acid as reference).

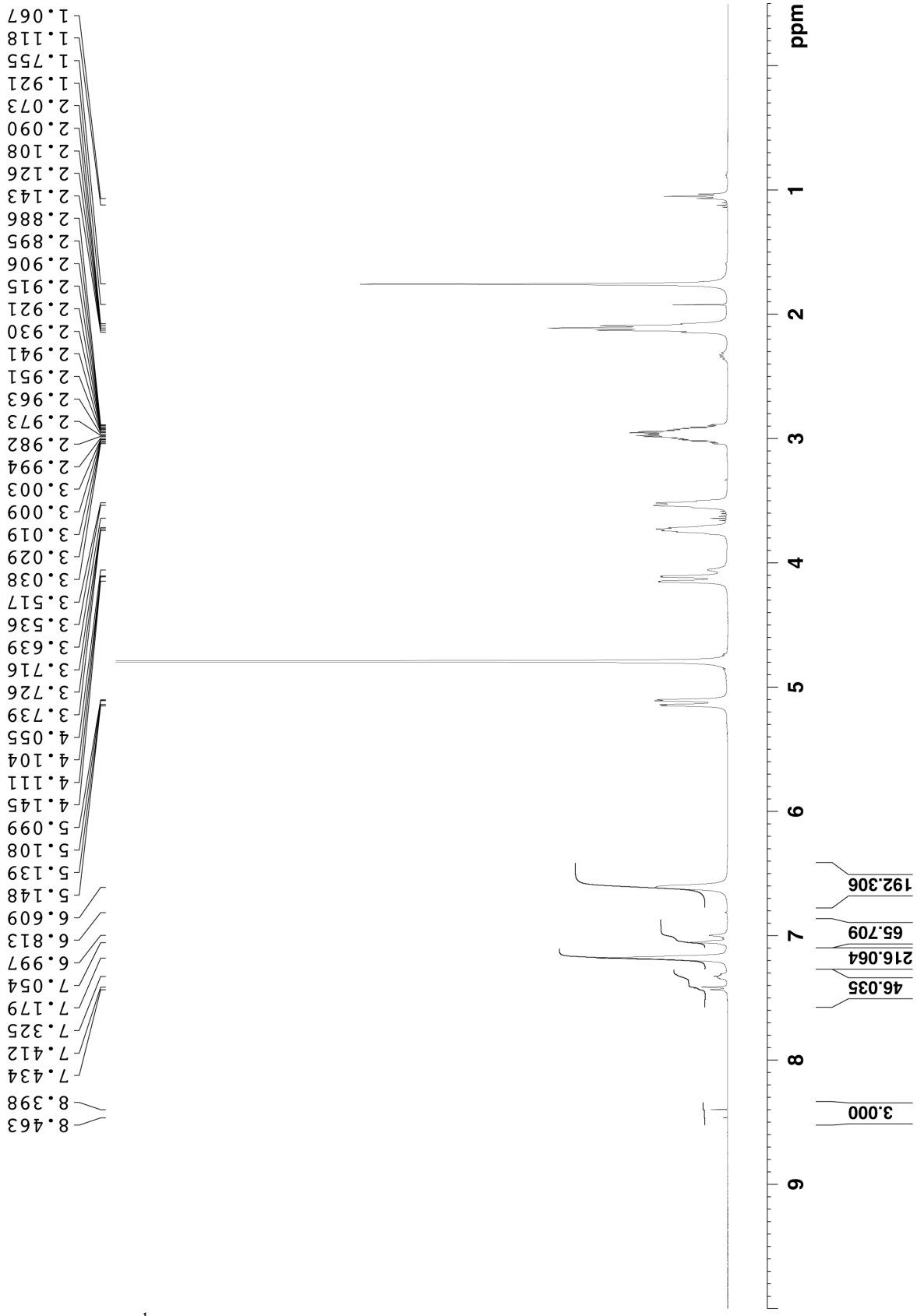

Figure S34. ^{1}H NMR recorded for camptothecin with **1b** (50 mM) (400 MHz, 20 mM NaD_2PO_4, pD 7.4, RT, 1,3,5 benzenetricarboxylic acid as reference).

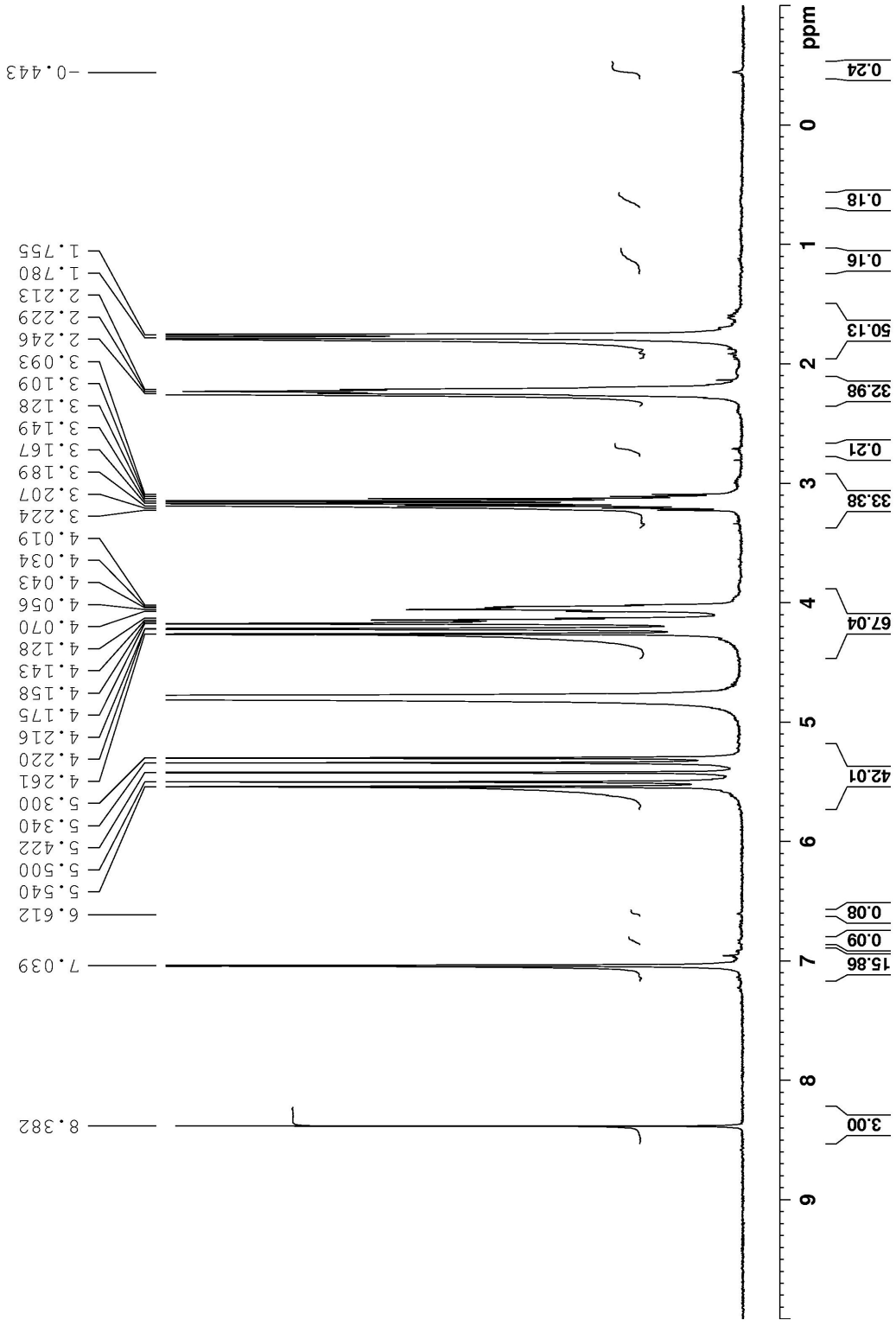

Figure S35. ^{1}H NMR recorded for estradiol with **3a** (10 mM) (400 MHz, 20 mM NaD_2PO_4, pD 7.4, RT, 1,3,5 benzenetricarboxylic acid as reference).

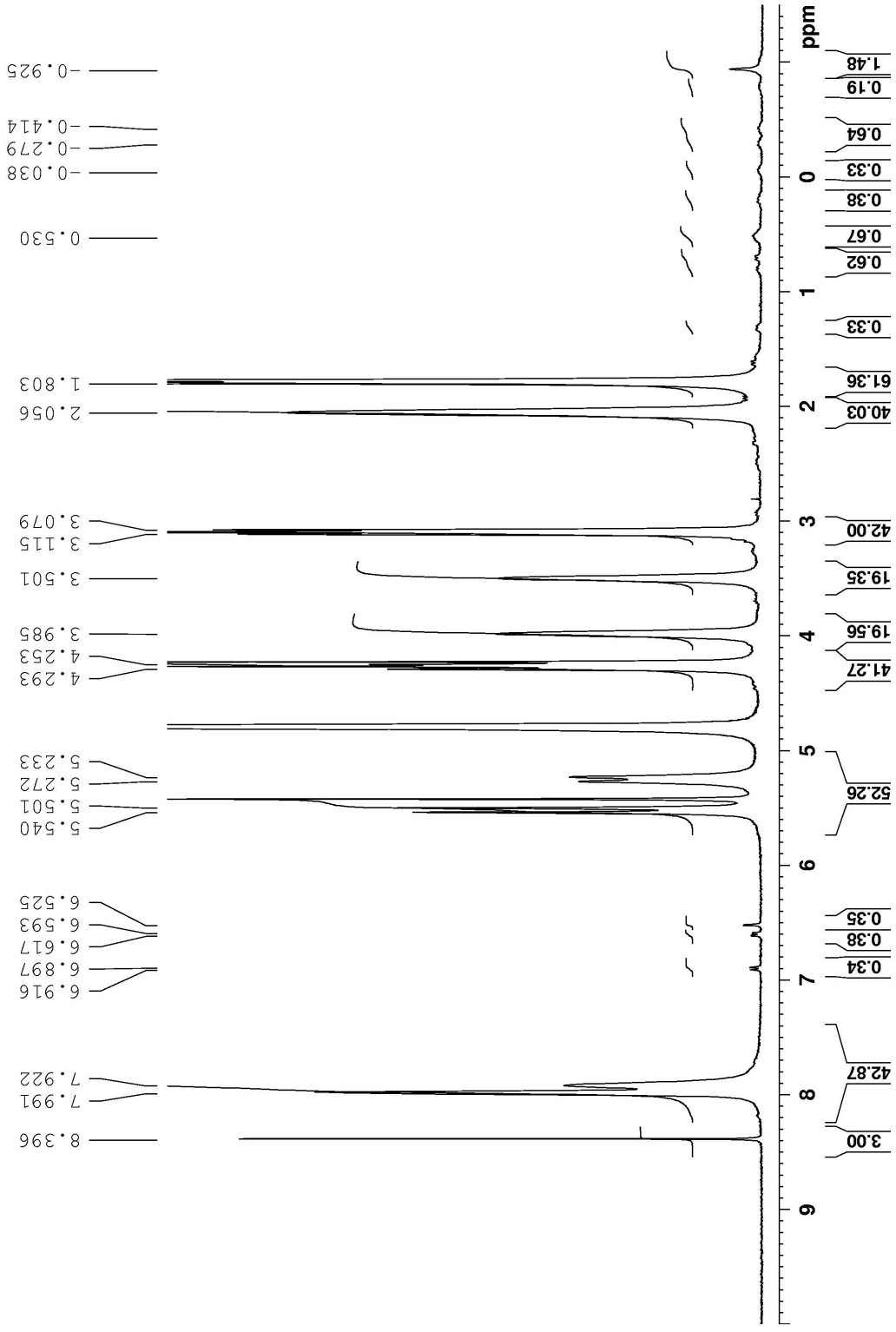

Figure S36. ^{1}H NMR recorded for estradiol with **3b** (10 mM) (400 MHz, 20 mM NaD_2PO_4, pD 7.4, RT, 1,3,5 benzenetricarboxylic acid as reference).

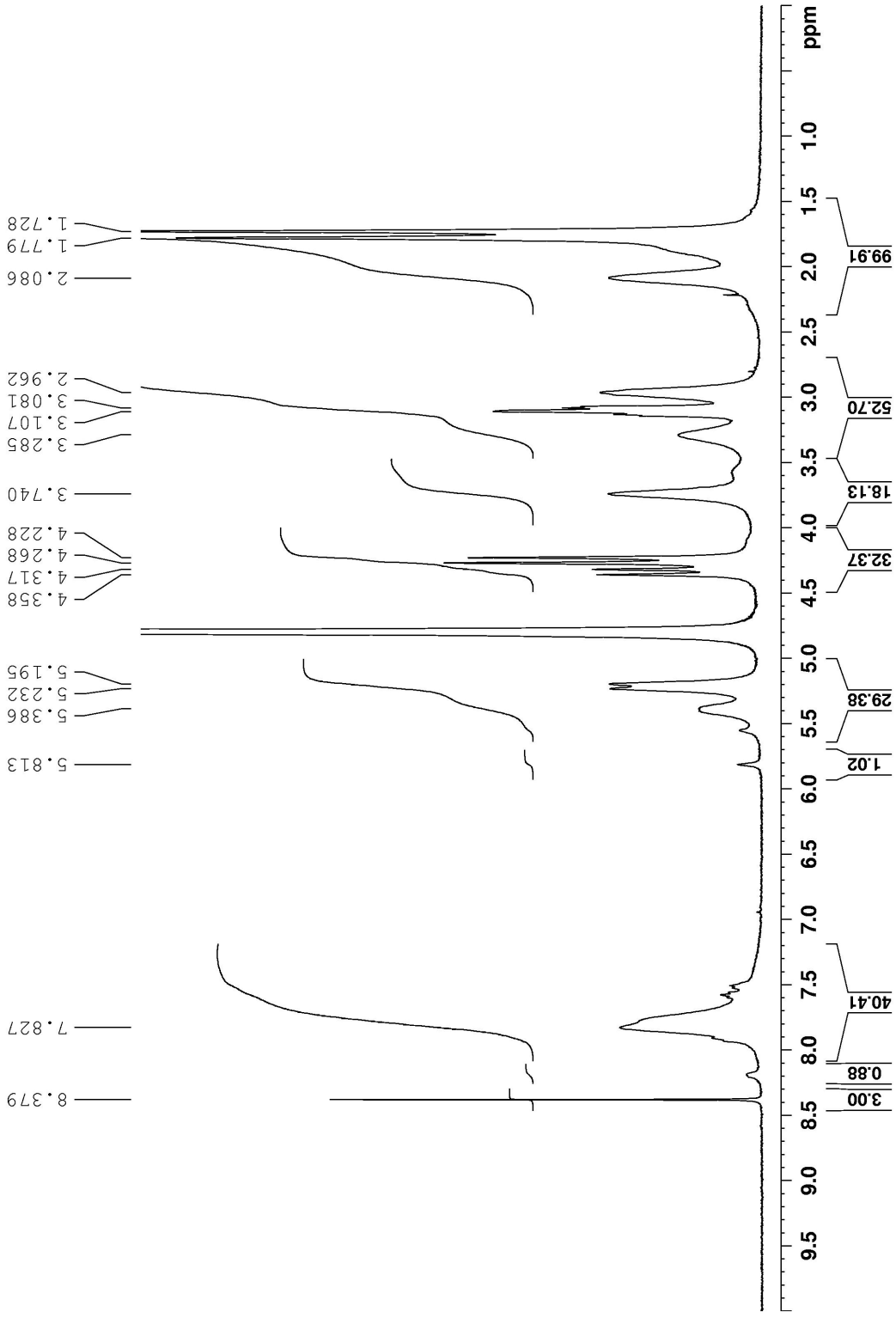

Figure S37. ^{1}H NMR recorded for ziprasidone with **2b** (10 mM) (400 MHz, 20 mM NaD_2PO_4, pD 7.4, RT, 1,3,5 benzenetricarboxylic acid as reference).

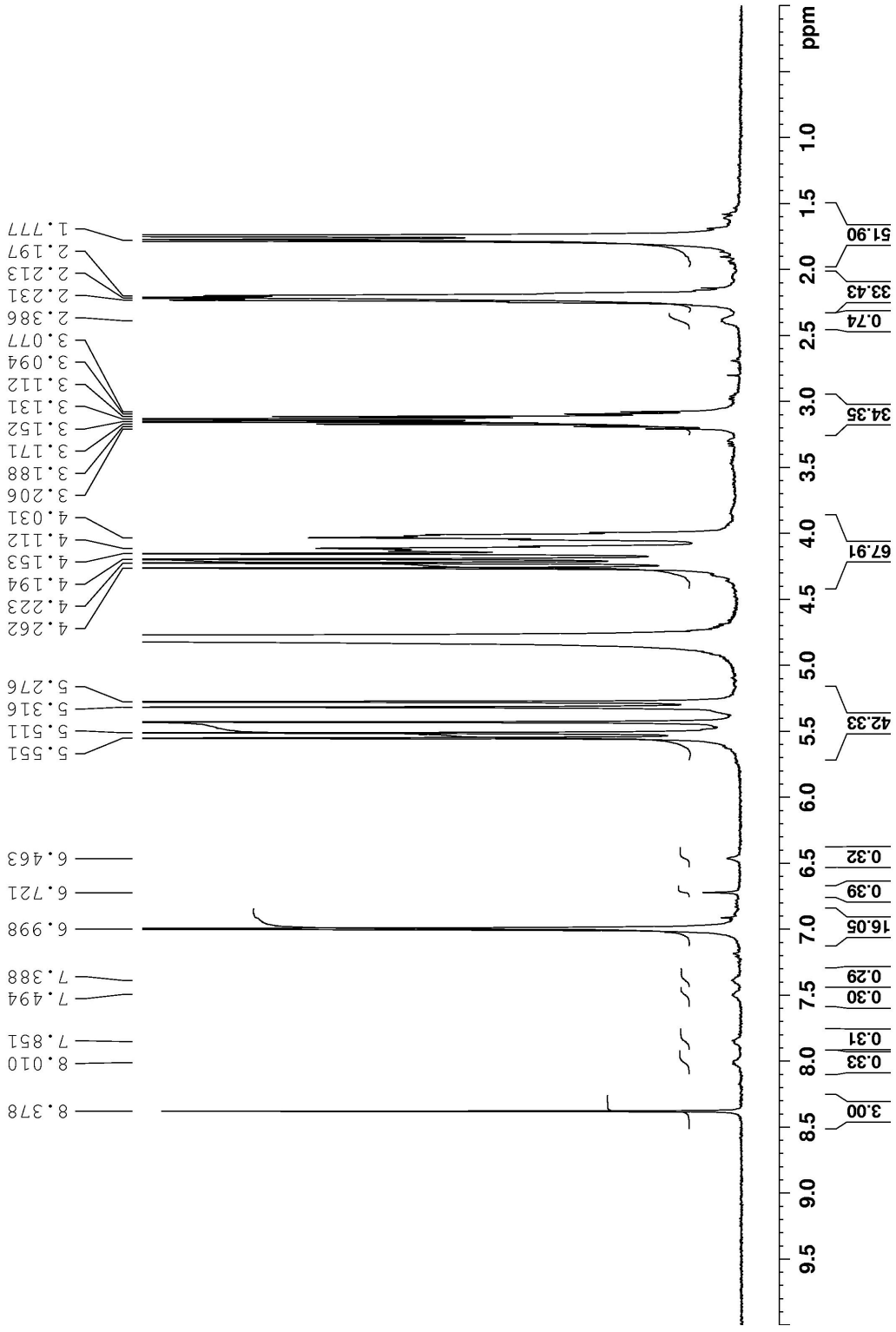

Figure S38. ^{1}H NMR recorded for ziprasidone with **3a** (10 mM) (400 MHz, 20 mM NaD_2PO_4, pD 7.4, RT, 1,3,5 benzenetricarboxylic acid as reference).

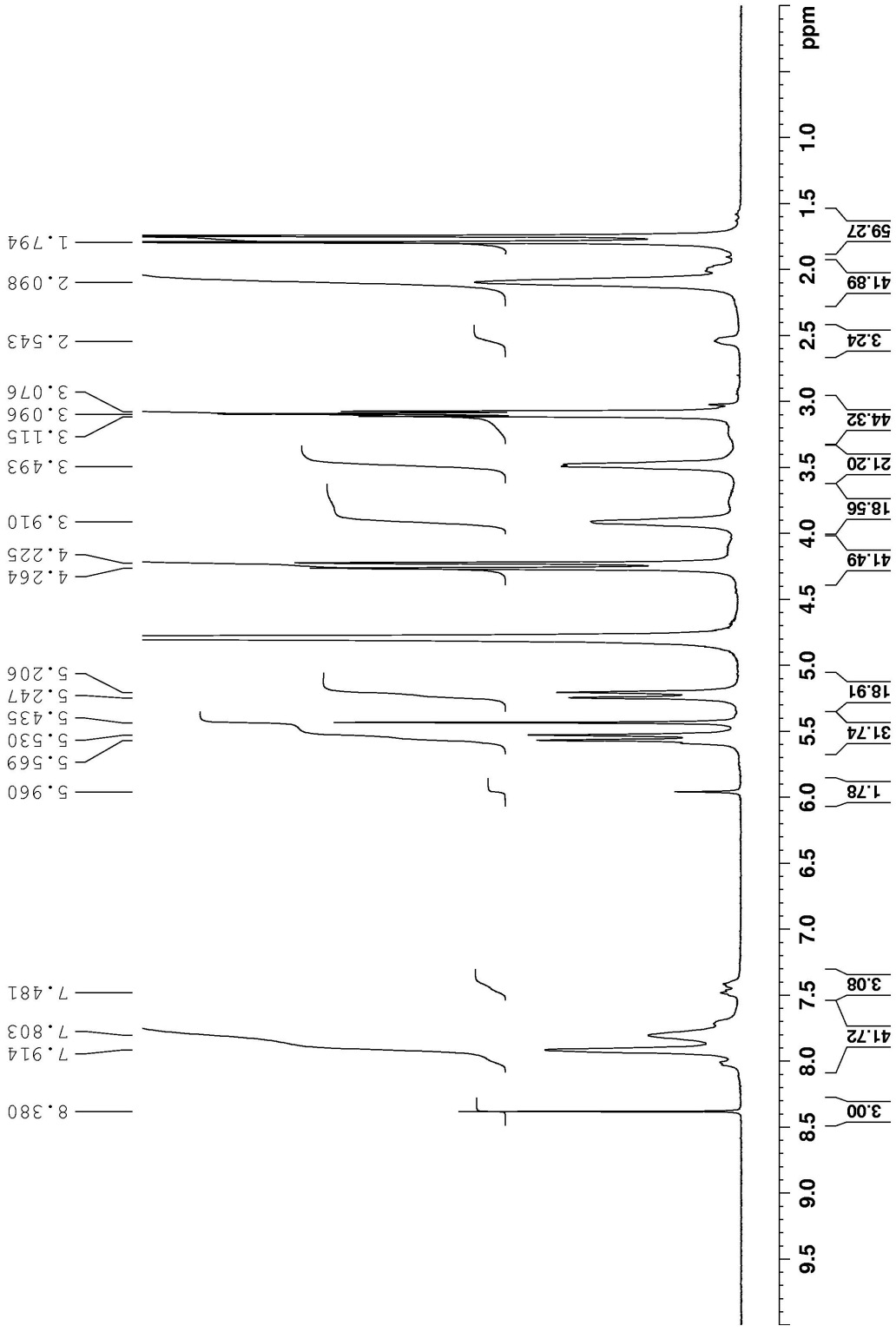

Figure S39. ^{1}H NMR recorded for ziprasidone with **3b** (10 mM) (400 MHz, 20 mM NaD_2PO_4, pD 7.4, RT, 1,3,5 benzenetricarboxylic acid as reference).

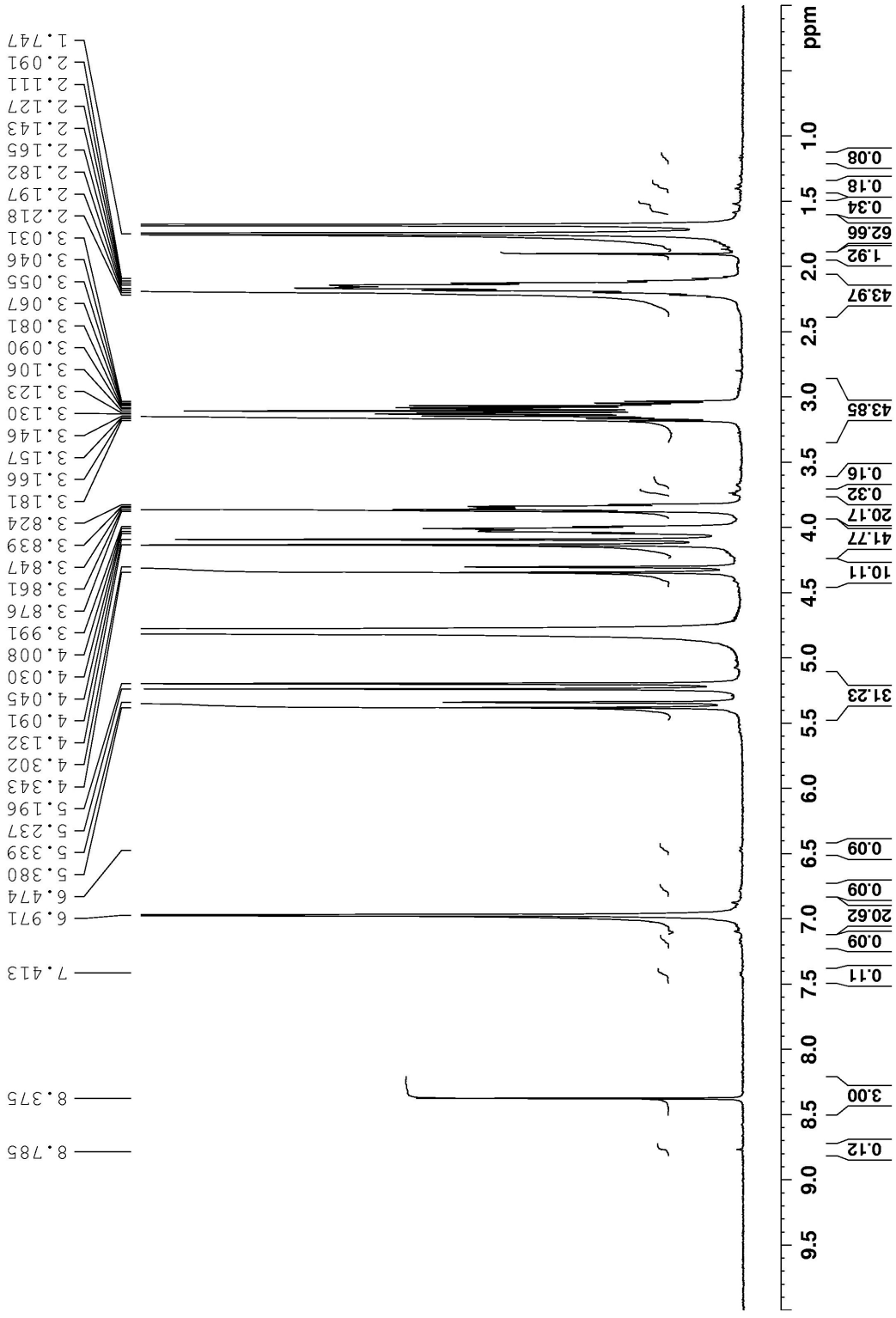

Figure S40. ^{1}H NMR recorded for PBS-1086 with **2a** (10 mM) (400 MHz, 20 mM NaD_2PO_4, pD 7.4, RT, 1,3,5 benzenetricarboxylic acid as reference).

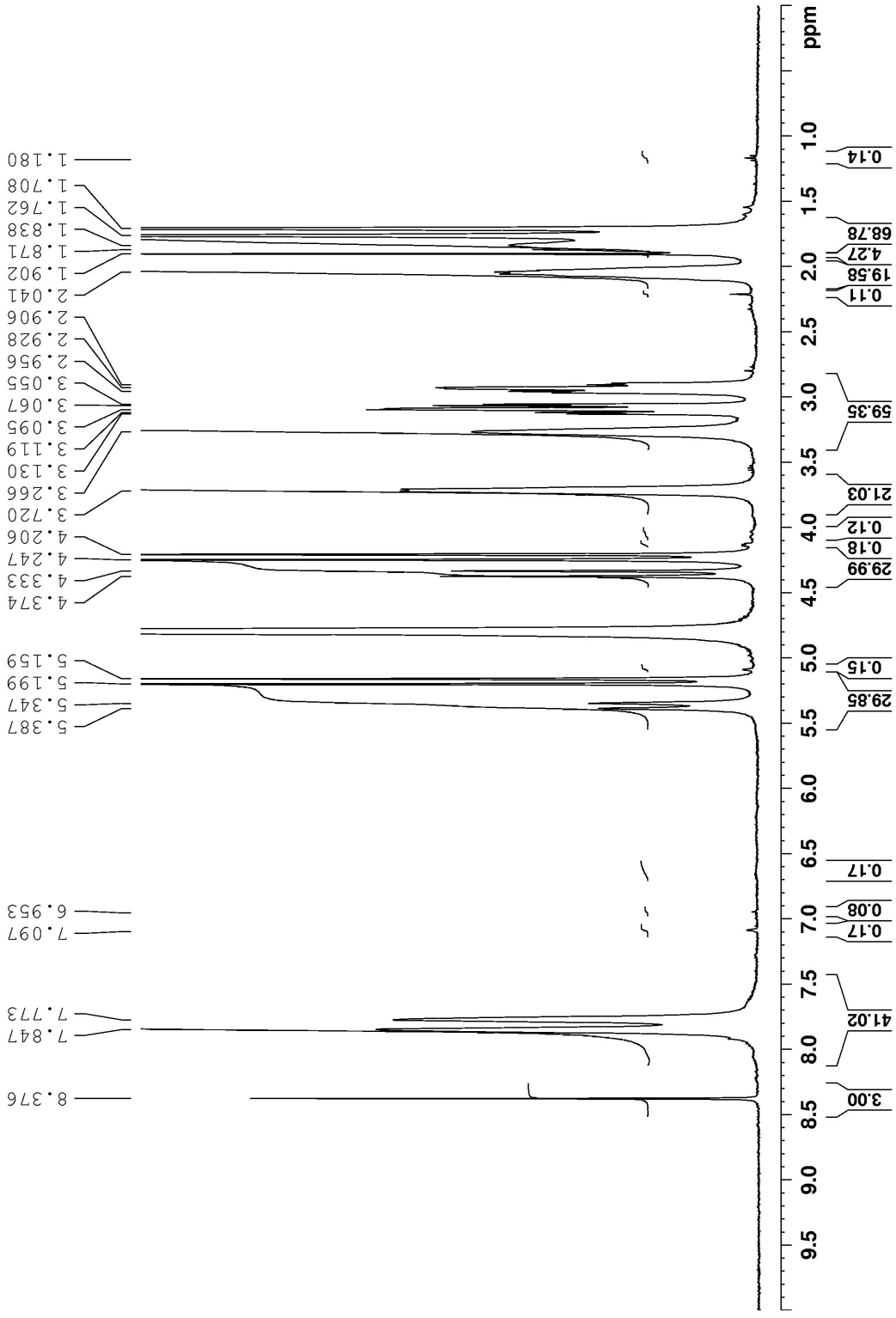

Figure S41. ^{1}H NMR recorded for PBS-1086 with **2b** (10 mM) (400 MHz, 20 mM NaD_2PO_4, pD 7.4, RT, 1,3,5 benzenetricarboxylic acid as reference).

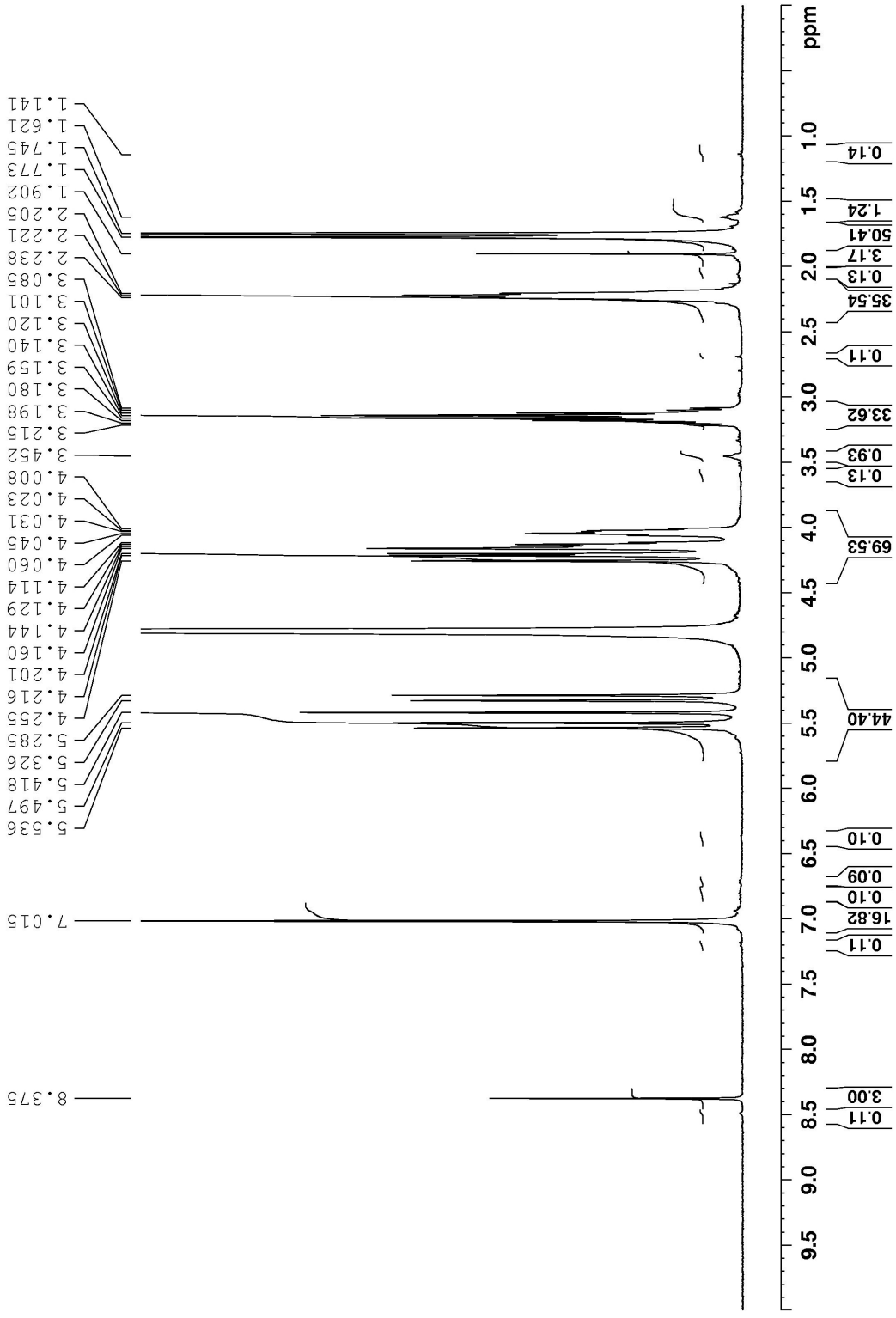

Figure S42. ^{1}H NMR recorded for PBS-1086 with **3a** (10 mM) (400 MHz, 20 mM NaD_2PO_4, pD 7.4, RT, 1,3,5 benzenetricarboxylic acid as reference).

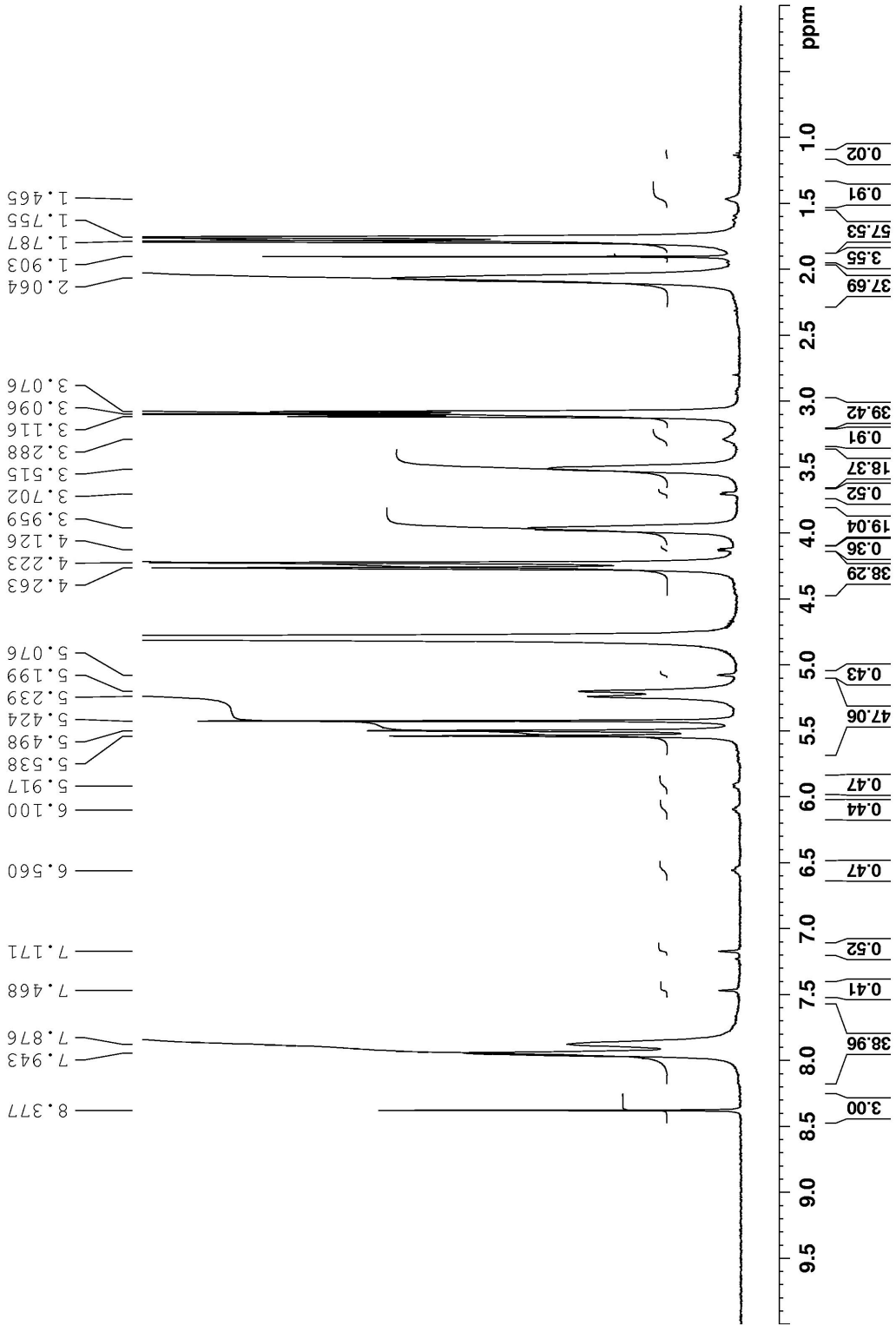

Figure S43. ^{1}H NMR recorded for PBS-1086 with **3b** (10 mM) (400 MHz, 20 mM NaD_2PO_4, pD 7.4, RT, 1,3,5 benzenetricarboxylic acid as reference).

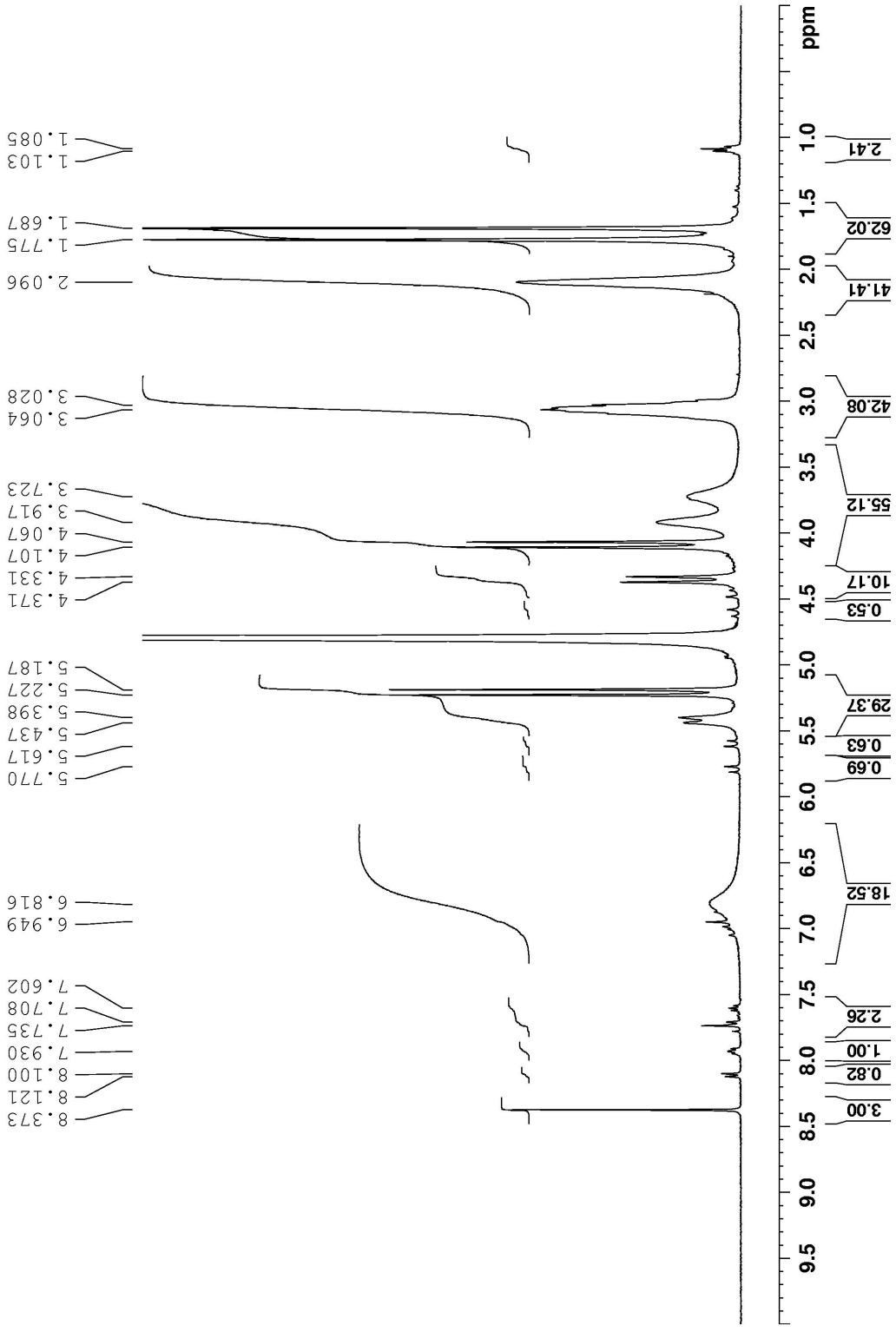

Figure S44. ^{1}H NMR recorded for camptothecin with **2a** (10 mM) (400 MHz, 20 mM NaD_2PO_4, pD 7.4, RT, 1,3,5 benzenetricarboxylic acid as reference).

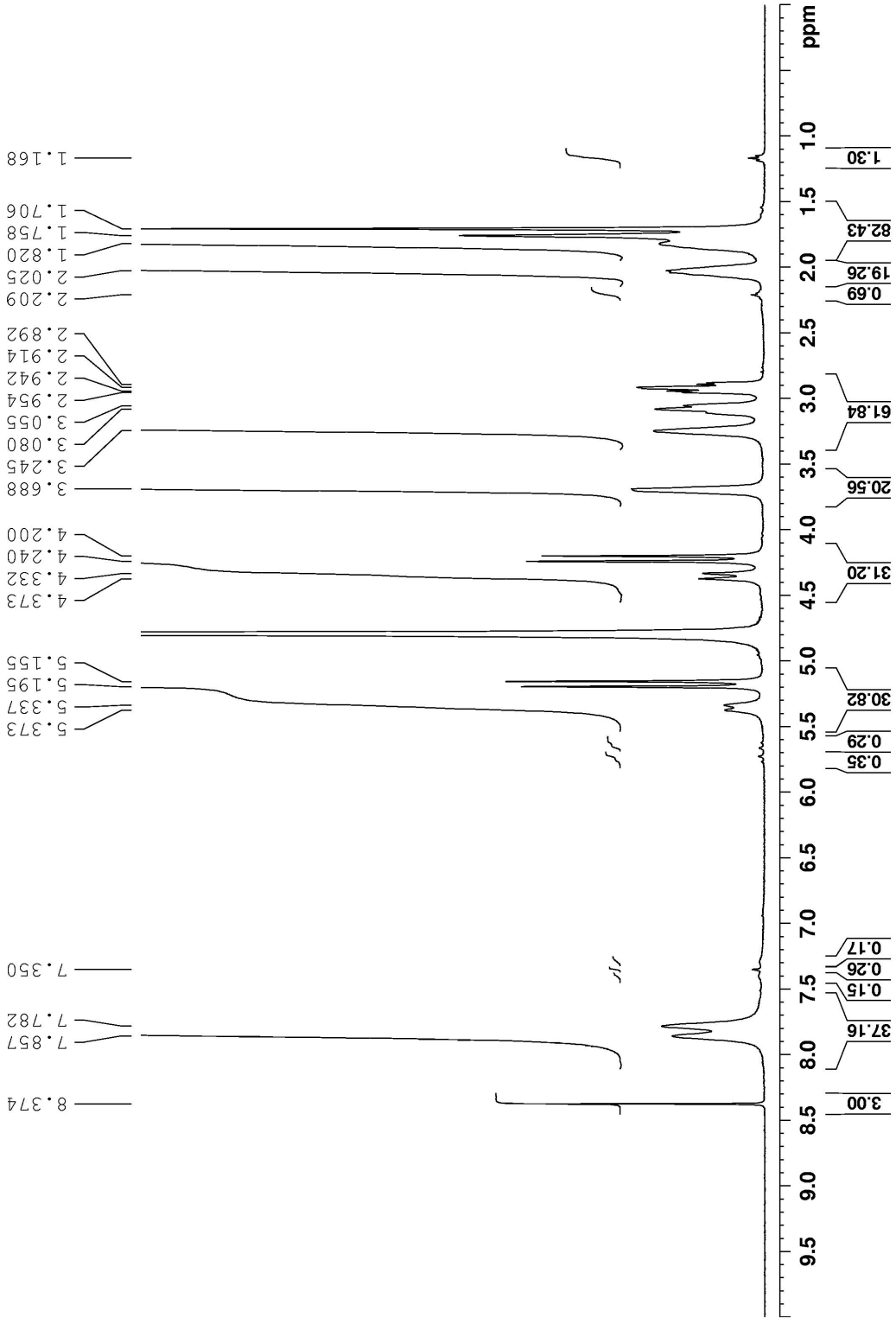

Figure S45. ^{1}H NMR recorded for camptothecin with **2b** (10 mM) (400 MHz, 20 mM NaD_2PO_4, pD 7.4, RT, 1,3,5 benzenetricarboxylic acid as reference).

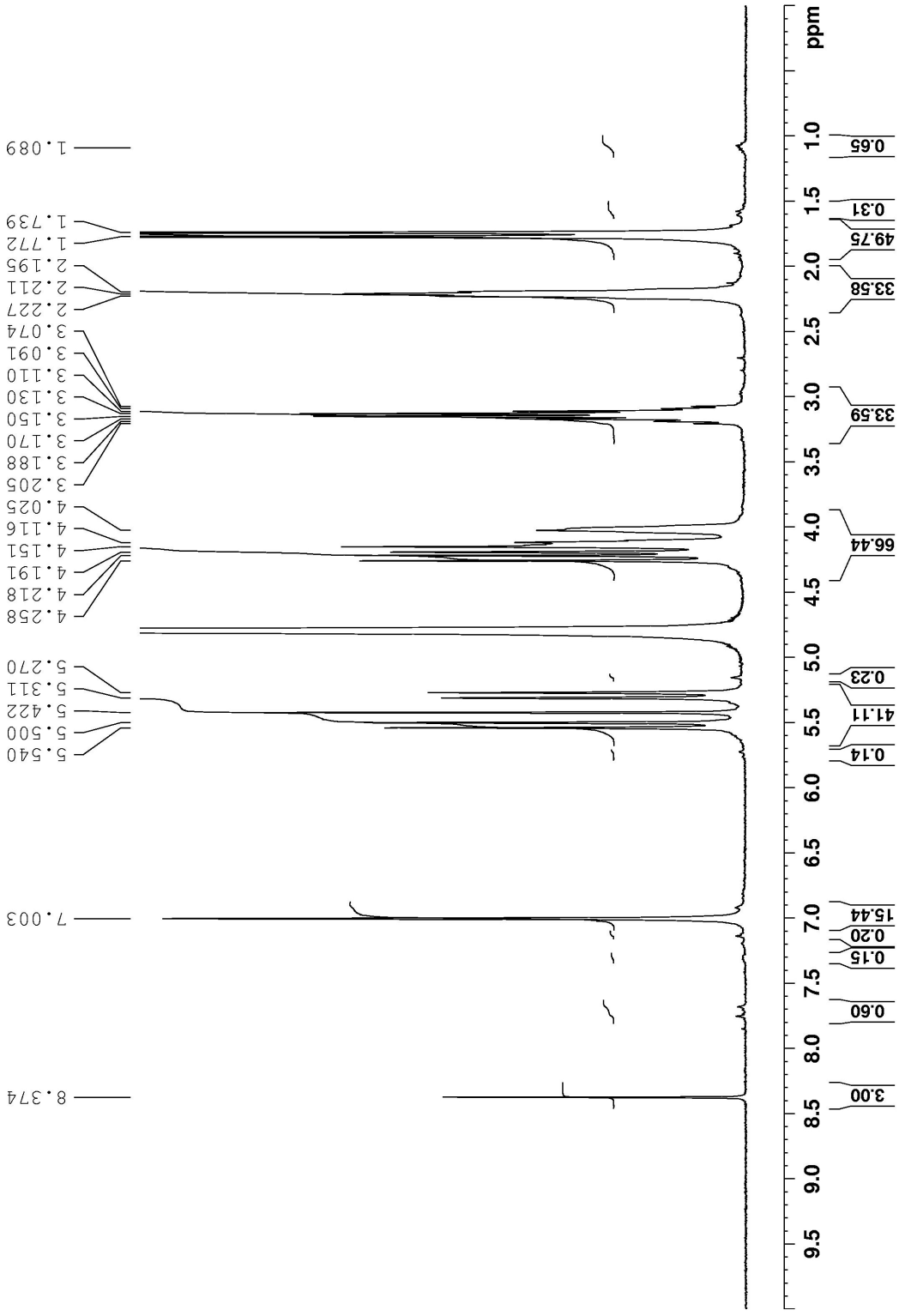

Figure S46. ^{1}H NMR recorded for camptothecin with **3a** (10 mM) (400 MHz, 20 mM NaD_2PO_4, pD 7.4, RT, 1,3,5 benzenetricarboxylic acid as reference).

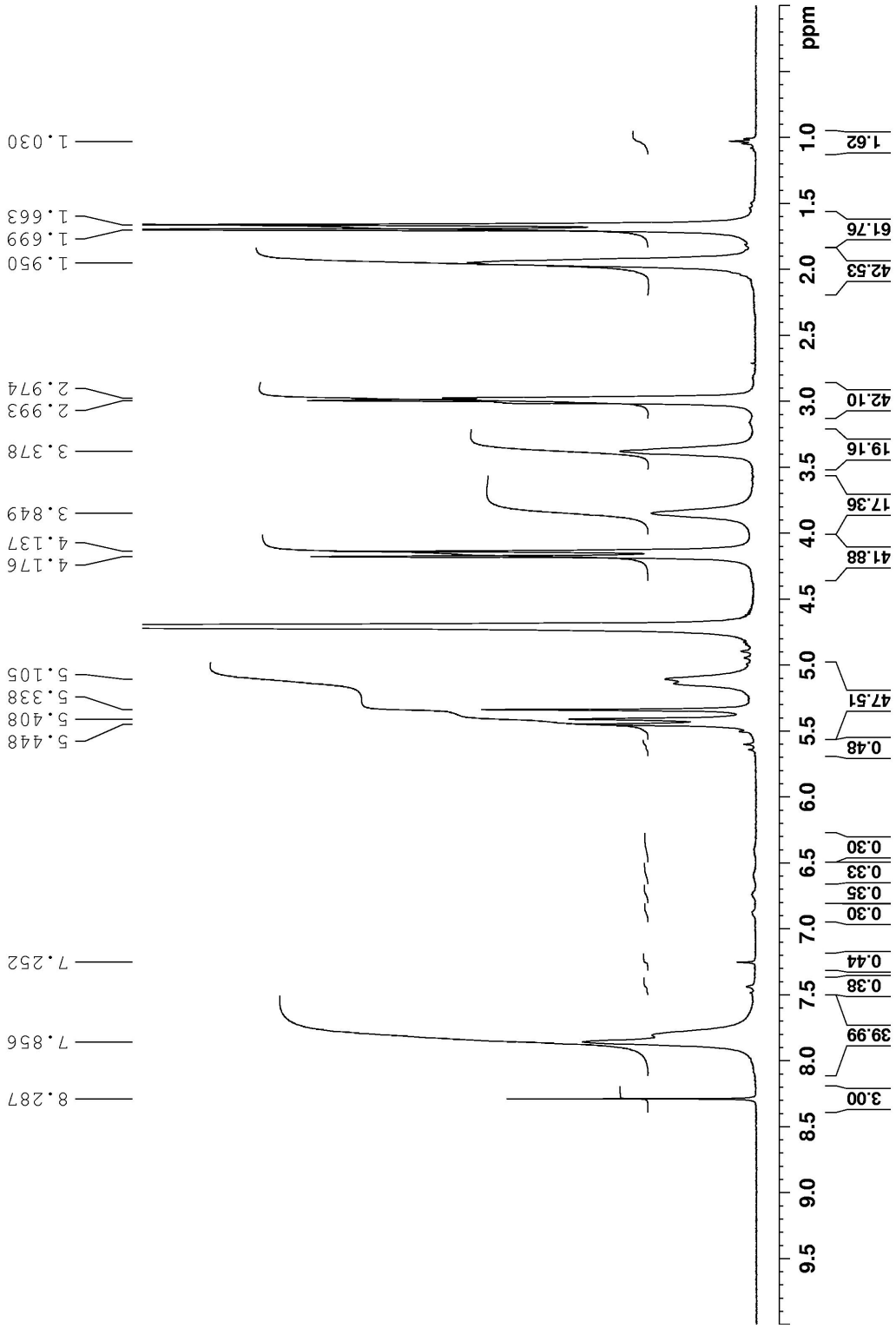

Figure S47. ^{1}H NMR recorded for camptothecin with **3b** (10 mM) (400 MHz, 20 mM NaD_2PO_4, pD 7.4, RT, 1,3,5 benzenetricarboxylic acid as reference).

Sample Error Analysis of Calculation for K_a. The K_a values were obtained from equation 1 and the uncertainty of K_a values was related to the intrinsic solubility values (S_0) and the slopes of the linear fit of the phase solubility diagrams (Slope). Here we give a sample calculation of the error analysis used to determine the uncertainty associated with the K_a value for **1b**•Camptothecin.

$$K_a = \frac{Slope}{S_0 \bullet (1 - Slope)} \tag{1}$$

Step 1 – Determination of the uncertainty of the intrinsic solubility of the water-insoluble drug and slopes of the linear fit of the phase-solubility diagrams. The slope values were obtained from the linear fit of the phase solubility diagrams and the uncertainty of the slope values were obtained as the standard deviation. The intrinsic solubility of the water-insoluble drug was measure with ^{1}H NMR for three times. The mean value of the samples was used as the S_0 value and the standard deviation of the samples was used as the uncertainty of S_0.

Step 2 – Determination of the uncertainty of K_a. We propagated the above uncertainty with K_a using equation 1 and equations 2 – 5 (Bevington "Data Reduction and Error Analysis for the Physical Sciences", McGraw-Hill, New York, 1969, page 61 – 62, eq. 4 – 11). Equation 2 delivers the uncertainty associated with the weighted product (x) of two values (u and v) (e.g. x = ± a u v). Similarly, equation 3 delivers the uncertainty for dividing two numbers (e.g. x = ± (a u) / v). We make the assumption that the fluctuations in u and v are not correlated (σ_{uv} = 0) which when substituted into equations 2 and 3 delivers equation 4. Equation 5 delivers the uncertainty for addition and subtraction (x = u ± v).

$$\frac{\sigma_x^{\,2}}{x^2} = \frac{\sigma_u^{\,2}}{u^2} + \frac{\sigma_v^{\,2}}{v^2} + 2\frac{\sigma_{uv}^{\,2}}{uv} \tag{2}$$

$$\frac{\sigma_x^{\,2}}{x^2} = \frac{\sigma_u^{\,2}}{u^2} + \frac{\sigma_v^{\,2}}{v^2} - 2\frac{\sigma_{uv}^{\,2}}{uv} \tag{3}$$

$$\frac{\sigma_x^{\,2}}{x^2} = \frac{\sigma_u^{\,2}}{u^2} + \frac{\sigma_v^{\,2}}{v^2} \tag{4}$$

$$\sigma_x^{\,2} = \sigma_u^{\,2} + \sigma_v^{\,2} \tag{5}$$

In this calculation, we break the calculation into three parts: 1) Subtracting (1 – Slope), 2) Multiplying (S_0•(1 – Slope)), and 3) Dividing Slope with the results in the previous part. From equation 5, we determined that $\sigma_{Slope} = \sigma_{(1\ -\ Slope)}$. From equation4 we can obtain the uncertainty of S_0•(1 – Slope) (equation 6).

$$\frac{\sigma_{S_0(1-Slope)}^{\,2}}{S_0(1-Slope)^2} = \frac{\sigma_{S_0}^{\,2}}{S_0^{\,2}} + \frac{\sigma_{Slope}^{\,2}}{(1-Slope)^2} \tag{6}$$

Meanwhile, from equation 4 we are able to calculate the uncertainty of K_a from equation 7.

$$\frac{\sigma_{K_a}^{\,2}}{K_a^{\,2}} = \frac{\sigma_{Slope}^{\,2}}{Slope^2} + \frac{\sigma_{S_0(1-Slope)}^{\,2}}{S_0^{\,2}(1-Slope)^2} \tag{7}$$

Substitution equation 6 into equation 7 gives equation 8.

$$\frac{\sigma_{K_a}^{\,2}}{K_a^{\,2}} = \frac{\sigma_{Slope}^{\,2}}{Slope^2} + \frac{\sigma_{S_0}^{\,2}}{S_0^{\,2}} + \frac{\sigma_{Slope}^{\,2}}{(1-Slope)^2} \tag{8}$$

Substitution of S_0 (54 (± 3.9) × 10^{-6} M), Slope (0.54 ± 0.0032) and K_a (2.2 × 10^4 M^{-1}) into equation 8 gives the $\sigma_{Ka} = 1.6 \times 10^3$ M^{-1}.

Binding Model (Self-association) implemented in Scientist™

```
// Micromath Scientist Model File
// self-association model for NMR
IndVars: conctot
DepVars: Deltaobs
Params: Ka, Deltasat, Deltazero
Ka = concBound/(concFree*concFree)
concTot=concFree + concBound/2
Deltaobs = Deltazero + (Deltasat - Deltazero) * (1/2*concBound/concTot)
//Constraints
0 < Ka
0 < concFree < concTot
0 < concBound < concTot
***
```

Binding Model (Self-association) for Global Fitting implemented in Scientist™

```
// Micromath Scientist Model File
IndVars: ConcHost
DepVars: CSA, CSB, CSC
Params: Ka, CSAzero, CSAsat, CSBzero, CSBsat, CSCzero, CSCsat
Ka = ConcHG/(ConcHfree*ConcGfree)
ConcHost=ConcHfree+ConcHG
0.0002=ConcGfree+ConcHG
CSA = CSAzero + ((CSAsat-CSAzero)*(ConcHG/0.0002))
CSB = CSBzero + ((CSBsat-CSBzero)*(ConcHG/0.0002))
CSC = CSCzero + ((CSCsat-CSCzero)*(ConcHG/0.0002))
0<ConcHfree<ConcHost
0<ConcGfree<0.0002
```